Repression of Lateral Organ Boundary Genes by PENNYWISE and POUND-FOOLISH Is Essential for Meristem Maintenance and Flowering in Arabidopsis[1][OPEN]

Madiha Khan, Laura Ragni[2], Paul Tabb, Brenda C. Salasini, Steven Chatfield[3], Raju Datla, John Lock, Xiahezi Kuai, Charles Després, Marcel Proveniers, Cao Yongguo, Daoquan Xiang, Halima Morin, Jean-Pierre Rullière, Sylvie Citerne, Shelley R. Hepworth*, and Véronique Pautot*

Department of Biology, Carleton University, Ottawa, Ontario, Canada K1S 5B6 (M.K., P.T., B.C.S., S.Ch., J.L., S.R.H.); Institut Jean-Pierre Bourgin, Unité Mixte de Recherche 1318 Institut National de la Recherche Agronomique-AgroParisTech, Bâtiment 2, Institut National de la Recherche Agronomique Centre de Versailles-Grignon, 78026 Versailles cedex, France (L.R., H.M., J.-P.R., S.Ci., V.P.); Plant Biotechnology Institute, National Research Council Canada, Saskatoon, Saskatchewan, Canada S7N 0W9 (R.D., C.Y., D.X.); Department of Biological Sciences, Brock University, St. Catharines, Ontario, Canada L2S 3A1 (X.K, C.D.); and Molecular Plant Physiology, Department of Biology, Faculty of Sciences, Utrecht University, CH–3584 Utrecht, The Netherlands (M.P.)

ORCID IDs: 0000-0002-0050-4001 (B.C.S.); 0000-0002-3526-7982 (J.L.); 0000-0001-7896-6049 (M.P.); 0000-0001-7144-1274 (D.X.); 0000-0001-5026-095X (S.Ci.); 0000-0002-6496-3792 (S.R.H.); 0000-0003-1808-5172 (V.P.).

In the model plant Arabidopsis (*Arabidopsis thaliana*), endogenous and environmental signals acting on the shoot apical meristem cause acquisition of inflorescence meristem fate. This results in changed patterns of aerial development seen as the transition from making leaves to the production of flowers separated by elongated internodes. Two related *BEL1-like* homeobox genes, *PENNYWISE* (*PNY*) and *POUND-FOOLISH* (*PNF*), fulfill this transition. Loss of function of these genes impairs stem cell maintenance and blocks internode elongation and flowering. We show here that *pny pnf* apices misexpress lateral organ boundary genes *BLADE-ON-PETIOLE1/2* (*BOP1/2*) and *KNOTTED-LIKE FROM ARABIDOPSIS THALIANA6* (*KNAT6*) together with *ARABIDOPSIS THALIANA HOMEOBOX GENE1* (*ATH1*). Inactivation of genes in this module fully rescues *pny pnf* defects. We further show that BOP1 directly activates *ATH1*, whereas activation of *KNAT6* is indirect. The *pny pnf* restoration correlates with renewed accumulation of transcripts conferring floral meristem identity, including *FD*, *SQUAMOSA PROMOTER-BINDING PROTEIN LIKE* genes, *LEAFY*, and *APETALA1*. To gain insight into how this module blocks flowering, we analyzed the transcriptome of *BOP1*-overexpressing plants. Our data suggest a central role for the *microRNA156-SQUAMOSA PROMOTER BINDING PROTEIN-LIKE-microRNA172* module in integrating stress signals conferred in part by promotion of jasmonic acid biosynthesis. These data reveal a potential mechanism by which repression of lateral organ boundary genes by PNY-PNF is essential for flowering.

Plant development relies on the activity of the shoot apical meristem (SAM) as a continuous source of founder cells for production of new leaves, shoots, and internodes throughout the life cycle (for review, see Aichinger et al., 2012). A tight balance between the allocation of cells to developing primordia and the perpetuation of pluripotent stem cells in the central zone maintains the SAM at a constant size. In Arabidopsis (*Arabidopsis thaliana*), the vegetative SAM produces leaves in a spiral phyllotaxy with dormant axillary meristems. In conjunction, internode elongation is repressed, resulting in a basal rosette. The transition to flowering is governed by internal and external signals that converge at the SAM to promote acquisition of inflorescence meristem (IM) fate (for review, see Amasino and Michaels, 2010; Srikanth and Schmid, 2011; Andrés and Coupland, 2012). This process, known as floral evocation, results in new patterns of growth at the shoot apex, including production of flowers, and an increase in stem elongation, called bolting. Lateral organ boundaries are specialized domains of restricted growth that separate meristem and organ compartments and produce axillary meristems (for review, see Aida and Tasaka, 2006; Tian et al., 2014). Early in the transition to flowering, the IM produces cauline leaves and axillary meristems that develop as secondary inflorescences. After several nodes, the IM ceases production of leaves, and axillary meristems develop as flowers.

Floral repressors in the SAM block meristem competence to flowering during vegetative stages of development. Major pathways for promotion of flowering work in two ways: by down-regulation of floral repressors in the meristem and by production of factors that promote IM and floral meristem identity (Bernier, 1988; Yant et al., 2010; Srikanth and Schmid, 2011). The

switch to flowering is governed by internal signals, including age, Suc content, and GA, in conjunction with external cues based on photoperiod, vernalization, ambient temperature, and responsiveness to light or stress stimuli (for review, see Srikanth and Schmid, 2011; Wang, 2014). Inputs from these different pathways converge to regulate a number of floral integrator genes, including *FLOWERING LOCUS T* (*FT*), which is a central component of the photoperiod response (Srikanth and Schmid, 2011; Andrés and Coupland, 2012). FT encodes a small phosphatidylethanolamine-binding protein that is synthesized in leaves and travels through phloem to the SAM (for review, see Corbesier et al., 2007; Jaeger and Wigge, 2007; Mathieu et al., 2007; Andrés and Coupland, 2012), where it interacts with the basic region/leucine zipper motif (bZIP) transcription factor FD to activate genes conferring inflorescence identity, including *SUPPRESSOR OF OVEREXPRESSION OF CONSTANS1* (*SOC1*)/*AGAMOUS-LIKE20* (*AGL20*), *AGL24*, and *FRUITFULL* (*FUL*; Abe et al., 2005; Teper-Bamnolker and Samach, 2005; Wigge et al., 2005). These factors in turn promote the expression of floral meristem identity genes *LEAFY* (*LFY*), *APETALA1* (*AP1*), and *CAULIFLOWER* (*CAL*), which confer floral fate (Bowman et al., 1993). In parallel, age-regulated down-regulation of *microRNA156* (*miR156*) stabilizes *mRNA* encoding SQUAMOSA PROMOTER BINDING PROTEIN-LIKE (SPL3), SPL4, and SPL5 transcription factors, which function with FT-FD to specify flower development by directly activating *AP1*, *LFY*, and *FUL* expression (Yamaguchi et al., 2009; Jung et al., 2012; Wang, 2014). The plant hormone GA is a positive regulator of flowering with function that is more pronounced under short days (SDs) when other regulatory pathways are inactive. Under SDs, GAs activate the transcription of *SOC1* and *LFY* in the shoot apex. Under long days (LDs), GA is not required for activation of *SOC1* but is important for activation of other transcripts at the shoot apex. Its targets include *SPL* genes, which are also directly activated by SOC1 and FD (Galvão et al., 2012; Porri et al., 2012). How these various pathways are integrated with stress signals is an area of active study (Yang et al., 2012; Heinrich et al., 2013; Hou et al., 2013; Diallo et al., 2014; Stief et al., 2014).

Members of the THREE-AMINO-ACID-LOOP-EXTENSION (TALE) class of homeodomain transcription factors constitute major regulators of meristematic activity. This family includes KNOTTED1-like (KNOX) and BEL1-like (BELL) or BEL1-LIKE HOMEODOMAIN (BLH) members, which function as heterodimers (for review, see Hamant and Pautot, 2010; Hay and Tsiantis, 2010). *SHOOT MERISTEMLESS* (*STM*), which is the founding member of the *KNOX* family in Arabidopsis, is required for SAM initiation and maintenance (Clark et al., 1996; Endrizzi et al., 1996; Long et al., 1996). Other *TALE* members, such as *BREVIPEDICELLUS* (*BP*)/*KNOTTED-LIKE FROM ARABIDOPSIS THALIANA1* (*KNAT1*), *KNAT6*, *PENNYWISE* (*PNY*; also known as *BELLRINGER*, *REPLUMLESS*, *VAAMANA*, or *LARSON*), *POUND-FOOLISH* (*PNF*), and *ARABIDOPSIS THALIANA HOMEOBOX GENE1* (*ATH1*) are expressed in the SAM and contribute redundantly with *STM* in meristem initiation and maintenance (Byrne et al., 2000; Belles-Boix et al., 2006; Rutjens et al., 2009).

PNY contributes to meristem maintenance and flowering with its closest relative, PNF (Smith et al., 2004). During vegetative development, the SAM in *pny pnf* mutants frequently terminates with development resuming from leaf-derived axillary meristems, a phenotype linked to reduced expression of *STM* (Smith et al., 2004; Ung et al., 2011; Ung and Smith, 2011). The *pny pnf* double mutant is also nonflowering. The *pny pnf* meristem changes shape in response to floral inductive signals, and inflorescence identity genes *SOC1* and *FUL* are up-regulated; however, *FT* levels are reduced, and floral meristem identity genes *LFY*, *AP1*, and *CAL* are not expressed (Smith et al., 2004; Kanrar et al., 2008). The basis of this phenotype is only partly understood. Ectopic expression of *LFY* in *pny pnf* mutants partially rescues flowering at axillary meristems, whereas ectopic expression of *FT* fails to rescue flowering and partially restores internode elongation at length, suggesting that FT requires PNY-PNF to initiate flower development (Kanrar et al., 2008). Additional data show that STM functions in association with PNY-PNF to specify flowers by promotion of *LFY* expression (Kanrar et al., 2006, 2008). This has led to the proposal that STM and PNY-PNF function together with flowering time products FT-FD and AGL24-SOC1 to initiate development of reproductive structures, flowers, and internodes (Smith et al., 2011). More recently, PNY-PNF were shown to promote the expression of SPL3, SPL4, and SPL5

[1] This work was supported by l'Oréal Canada (Women in Science Award to M.K.), the France-Canada Research Fund (M.K.), the European Union (Early Stage Training Site Versailles-Evry Research Training [VERT] Grant no. MEST–CT–2004–7576 VERT to L.R.), the European Marie-Curie (FP6) Program (L.R.), a Douglas Anglin Scholarship (to B.C.S.), and the Natural Sciences and Engineering Research Council (Accelerator and Discovery Grant nos. 429440 to C.D. and 251163 to C.D. and Discovery Grant no. 327195 to S.R.H.).

[2] Present address: Center for Plant Molecular Biology, Zentrum für Molekularbiologie des Pflanzen Developmental Genetics, University of Tübingen, Auf der Morgenstelle 32, D–72076 Tuebingen, Germany.

[3] Present address: University of Toronto Mississauga, 3359 Mississauga Road, Mississauga, ON, Canada L5L 1C6.

* Address correspondence to shelley_hepworth@carleton.ca and pautot@versailles.inra.fr.

The author responsible for distribution of materials integral to the findings presented in this article in accordance with the policy described in the Instructions for Authors (www.plantphysiol.org) is: Shelley R. Hepworth (shelley_hepworth@carleton.ca).

All authors made essential contributions to the project; M.K., L.R., P.T., and B.C.S. performed most of the experiments; J.L. analyzed the *ATH1p:GUS* lines; S.Ch., R.D., C.Y., and D.X. provided the microarray data; X.K. and C.D. performed the ChIP assays; H.M. performed the in situ analysis with V.P.; S.Ci. measured the JA content and provided technical assistance to V.P.; J.-P.R. provided technical assistance to V.P.; M.P. participated by communicating unpublished results; S.R.H. and V.P. conceived the project, designed the experiments, did some of the experiments, analyzed the data, and wrote the article.

[OPEN] Articles can be viewed without a subscription.
www.plantphysiol.org/cgi/doi/10.1104/pp.15.00915

transcription factors that direct activation of floral meristem identity genes in parallel with FT-FD (Lal et al., 2011). Compatible with this, miR156 is up-regulated in *pny pnf* apices. Ectopic expression of *SPL4* in *pny pnf* restores accumulation of *LFY* and *AP1* transcripts and partially restores flower formation (Lal et al., 2011). However, none of these mechanisms identified to date fully explain the basis of *pny pnf* meristem defects.

In addition to roles in the SAM, these factors have distinct functions in establishing inflorescence architecture. Significant reorganization of *KNOX-BELL* gene expression occurs at the transition to flowering in correlation with new patterns of aerial development (Lincoln et al., 1994; Byrne et al., 2003; Smith and Hake, 2003; Smith et al., 2004; Proveniers et al., 2007; Gómez-Mena and Sablowski, 2008). PNY and BP maintain proper internode patterning through the regulation of cell wall remodeling proteins (Mele et al., 2003; Etchells et al., 2012). Mutations in *bp* cause short internodes and downward-pointing flowers, whereas mutations in *pny* cause irregular elongation of internodes, leading to clusters of flowers on the primary stem with phenotypes enhanced in the double mutant. Studies in Arabidopsis have identified the joint activities of BLADE-ON-PETIOLE (BOP) Broad Complex, Tramtrack, and Bric-a-brac (BTB)-ankyrin coactivators and TALE homeodomain transcription factors as important in maintaining lateral organ boundaries (for review, see Hamant and Pautot, 2010; Hay and Tsiantis, 2010; Khan et al., 2014). BP and PNY restrict expression of lateral organ boundary genes *BOP1/2*, *KNAT2*, *KNAT6*, and *ATH1* to boundaries at the base of the floral shoot in controlling growth patterns in the inflorescence (Ragni et al., 2008; Khan et al., 2012a, 2012b; Zhao et al., 2015). These studies revealed that BOP1/2 promote ATH1 and KNAT6 which form a module that opposes BP-PNY activity in regulating inflorescence architecture (Rutjens et al., 2009; Khan et al., 2012a, 2012b, 2014; Li et al., 2012).

Here, we investigated the interaction of BOP1/2 with TALE members in flower formation. Our studies reveal that PNY and PNF repress the lateral organ boundary genes BOP1/2 and transcriptional targets *ATH1* and *KNAT6* to maintain meristem integrity and flowering. Inactivation of genes in this module fully rescues *pny pnf* defects in meristem maintenance, internode elongation, and flowering. To gain insight into how this module blocks flowering, we analyzed the transcriptome of *BOP1*-overexpressing plants. Our data indicate a role for stress signaling by promotion of jasmonic acid (JA) as a potential mechanism for counteracting flowering, including responsiveness to GA acting in part through the *miR156-SPL-miR172* module.

RESULTS

Inactivation of *BOP1/2*, *KNAT6*, or *ATH1* Rescues Meristem Maintenance, Internode Elongation, and Flowering Defects in *pny pnf*

Previously, we showed that misexpression of boundary genes *BOP1/2*, *KNAT6*, and *ATH1* in *bp* and *pny* internodes perturbs inflorescence architecture through localized restriction of growth. Inactivation of genes in this module fully rescues *pny* defects in internode elongation and phyllotaxy, but inactivation of *KNAT2* has no such effect (Ragni et al., 2008; Khan et al., 2012a, 2012b). We anticipated that antagonistic functions of these same genes might cause *pny pnf* defects. The *pnf* single mutant has no obvious phenotype. The *pny* mutant has a functional SAM, but apical dominance is reduced, flowering is delayed, and organs are clustered on the primary stem because of irregular internode elongation. In *pny pnf*/+ hemizygous plants, these defects are enhanced, and stem-pedicel fusions occur (Smith and Hake, 2003; Supplemental Fig. S1, A–G). In *pny pnf* double mutants, the SAM terminates after the initiation of three to five leaves in a majority of seedlings (Smith et al., 2004; Rutjens et al., 2009). Lateral meristems in the axil of rosette leaves support the continued production of leaves, but flowering and internode elongation are blocked (Smith et al., 2004; Rutjens et al., 2009; Lal et al., 2011). To determine if *BOP1/2*, *KNAT/6*, and *ATH1* are required in generating *pny pnf* defects, we constructed *bop1 bop2 pny pnf*, *ath1 pny pnf*, *knat2 pny pnf*, *knat6 pny pnf*, and *knat6 knat2 pny pnf* mutants. We first tested for rescue of *pny pnf* defects in SAM maintenance. Previous studies using the *ath1-1* allele indicated that SAM arrest in triple mutants with *pny pnf* is markedly enhanced, likely because of the depletion of BELL-STM functional complexes (Rutjens et al., 2009). Here, we repeated the analysis with *ath1-3*, which unlike *ath1-1* and *ath1-4* alleles, produces no full or partial mutant transcript (Supplemental Fig. S2). Although 57.7% of *pny pnf* plants showed a meristem arrest, no such arrest was observed in *ath1-3 pny pnf* mutants ("Materials and Methods"; Fig. 1). Meristem function was also rescued by *bop1 bop2* and *knat6* mutations but not by inactivation of *KNAT2* (Fig. 1). These data suggest that PNY-PNF/STM antagonizes the activity of lateral organ boundary genes to maintain stem cell identity. Flower formation, internode elongation, and organ fusion defects were also rescued in *bop1 bop2 pny pnf* and *knat6 pny pnf* or *ath1-3 pny pnf* triple mutants compared with *pny pnf* and/or *pny pnf*/+ plants (Fig. 2, A–H; Supplemental Fig. S3). Quantitative phenotypic analyses showed that inflorescence architecture of *bop1 bop2 pny pnf*, *ath1 pny pnf*, and *knat6 pny pnf* mutants was similar to that of wild-type plants (Supplemental Fig. S4). In contrast, *knat2 pny pnf* mutants remained nonflowering (Fig. 2I).

Overexpression studies further support a role for *BOP1/2*, *ATH1*, and *KNAT6* in the same genetic pathway. Plants that overexpress *BOP1/2* are late flowering with shortened internodes and clustered fruits similar to *pny* and *pny pnf*/+ mutants (Supplemental Fig. S1, A–C; Norberg et al., 2005; Ha et al., 2007; Khan et al., 2012b). Plants overexpressing *ATH1* and occasionally, *KNAT6* have similar defects that mimic the inflorescence architecture of *pny* and *pny pnf*/+ mutants (Supplemental Fig. S1, B–I; Proveniers et al., 2007; Gómez-Mena and Sablowski, 2008; Shi et al., 2011). The

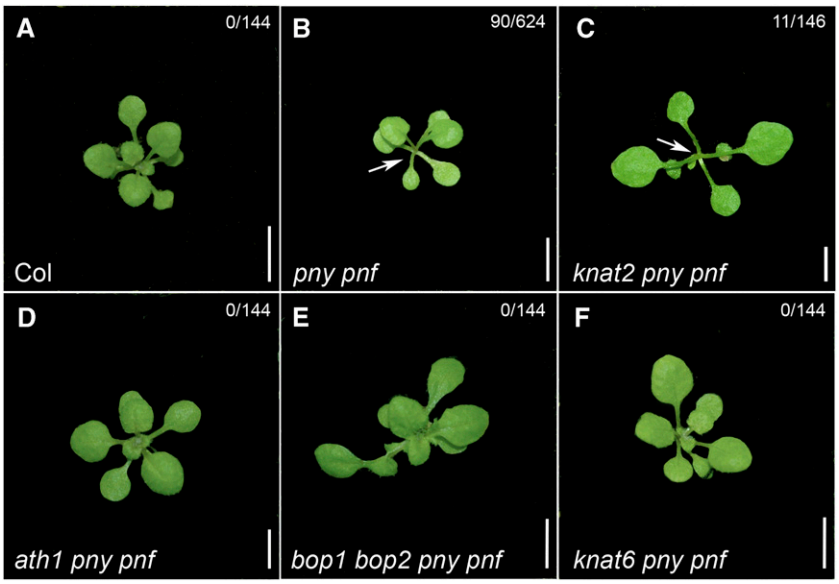

Figure 1. Inactivation of *BOP1/2*, *ATH1*, and *KNAT6* rescues *pny pnf* meristem arrest. Plants were grown under SDs. Numbers of plants showing a meristem arrest on day 25 are indicated at the upper right. A, Col-0 plant. The SAM produces leaves. B, *pny pnf* mutant showing a meristem arrest; 90 of 156 (57.7%) of expected *pny pnf* mutants in a *pny pnf/+* segregating population (n = 624) showed SAM arrest (arrow). C, *knat2 pny pnf* triple mutant (identical to *pny pnf* mutant); 11 of 36.5 (30.1%) of expected *knat2 pny pnf* triple mutants in a *knat2 pny pnf/+* segregating population (n = 146) showed SAM arrest (arrow). D, *ath1 pny pnf* triple mutant (no meristem arrest). E, *bop1 bop2 pny pnf* quadruple mutant (no meristem arrest). F, *knat6 pny pnf* triple mutant (no meristem arrest). Bars = 5 mm.

most severe *KNAT6* transgenic lines were strongly inhibited in their development and failed to flower (Supplemental Fig. S1, J and K). Collectively, these data indicate that PNY-PNF plays no essential function in meristem/boundary maintenance, internode elongation, and flowering beyond repression of BOP1/2 and ATH1/KNAT6.

BOP1/2, *ATH1*, and *KNAT2/6* Expression Domains Are Expanded in *pny pnf* Apices

Inflorescence defects in *pny* mutants correlate with an expanded pattern of expression for *BOP1/2*, *ATH1*, and *KNAT2/6* in internodes (Ragni et al., 2008; Khan et al., 2012a, 2012b). We therefore examined the expression patterns of these genes in *pny pnf* apices. In wild-type apices, *BOP2* transcripts accumulate in the adaxial domain of floral meristems until late stage 2, when expression shifts to the boundary with the cryptic bract. Expression is found in the boundary domains of older flowers (Fig. 3A; Xu et al., 2010). *ATH1* transcripts are expressed in incipient floral primordia and the dome of stage 2 floral primordia in a pattern similar to *KNAT2*. *KNAT6* transcripts are localized to boundary domains flanking the IM and in flowers also overlapping with *KNAT2* (Fig. 3, B–D). In *pny pnf* apices, the domain of expression for all of these genes expands into the central and rib zones of the meristem (Fig. 3, E–H). This was also observed for *BOP1* using a *BOP1-GUS* line (Supplemental Fig. S5). Misexpression of these genes likely begins during the vegetative stage based on analysis of *BOP2:GUS* lines (data not shown), consistent with SAM structural defects (Ung et al., 2011). Little or no misexpression was observed in *pny* or *pnf* control apices (Supplemental Fig. S6). These data confirm that *pny pnf* defects are caused by misexpression of *BOP1/2*, *ATH1*, and *KNAT6* in the meristem. We next examined regulatory interactions between these genes in the pathway.

ATH1 Is a Direct Target of BOP1

BOP1/2 was previously shown to promote the expression of *ATH1* and *KNAT6* and require these activities to exert changes in inflorescence (Khan et al., 2012a, 2012b). To test if *ATH1* and/or *KNAT6* are immediate transcriptional targets of BOP1/2, we used a transgenic line expressing a translational fusion of BOP1 to the steroid-binding domain of the rat glucocorticoid receptor (GR; Lloyd et al., 1994). This dexamethasone (DEX)-inducible system was used previously to show that BOP1 directly activates the transcription of *ASYMMETRIC LEAVES2* in leaves (Jun et al., 2010). Function of the BOP1-GR fusion protein was confirmed by expressing it under the control of a *BOP1* native promoter and observing efficient complementation of *bop1 bop2* leaf and abscission defects upon addition of DEX (Supplemental Fig. S7). Direct regulation of *ATH1* and/or *KNAT6* was tested using the BOP1-GR fusion protein expressed in wild-type plants under the control of a double 35S promoter. *D35S:BOP1-GR* plants treated with DEX for 4 weeks had shortened internodes and clustered fruits similar to *bop1-6D* mutants, which constitutively overexpress *BOP1* (Fig. 4, A–D; Norberg et al., 2005). Transcripts for *ATH1* were increased 13.29-fold and transcripts for *KNAT6* were increased 2.59-fold in *bop1-6D* internodes compared with the wild type (Fig. 4E). Similarly, *D35:BOP1-GR* plants treated with DEX for 4 weeks showed a 6-fold up-regulation of *ATH1* transcript (Fig. 4E). After 2 and 4 h of DEX treatment, transcript levels for *ATH1* were at least 2-fold higher, but *KNAT6* transcript levels showed no increase relative to mock-treated control plants (Fig. 4F; 24-h time point not shown). Rapid activation of *ATH1* suggested that its

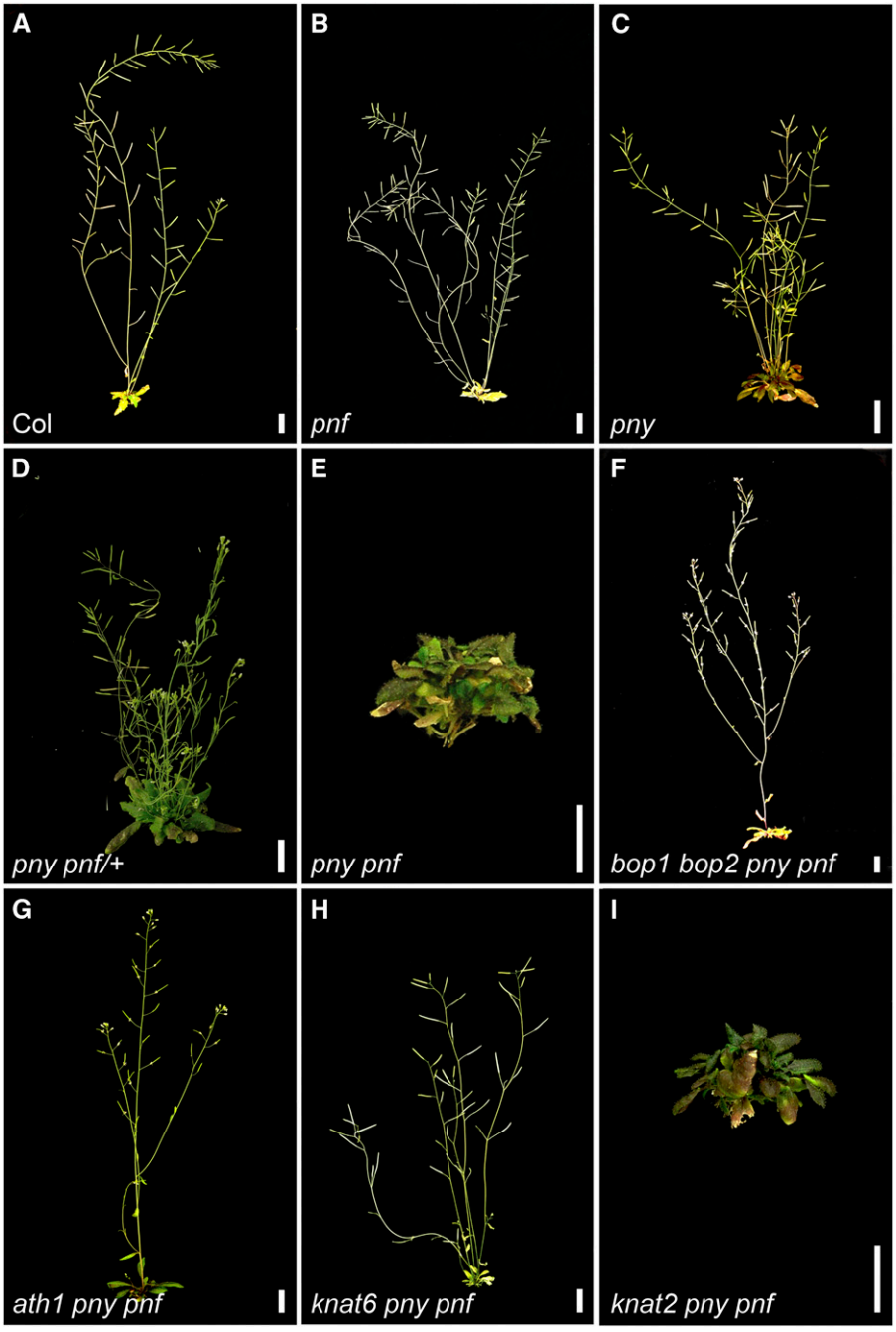

Figure 2. Inactivation of *BOP1/2*, *ATH1*, and *KNAT6* rescues internode and flower formation in *pny pnf* mutants. Representative 8-week-old plants are shown. A, Col-0 plant. B, *pnf* mutant showing a wild-type phenotype. C, *pny* mutant showing partial loss of apical dominance, short stature, and clusters of siliques. D, *pny pnf/+* hemi mutant showing partial loss of apical dominance, short stature, clusters of siliques, and stem/pedicel fusion defects (Supplemental Fig. S1). E, *pny pnf* double mutant (nonflowering). F, *bop1 bop2 pny pnf* quadruple mutant (similar to *bop1 bop2*). Inactivation of *BOP1* and *BOP2* in *pny pnf* rescues internode elongation and flowering. G, *ath1 pny pnf* triple mutant (similar to *ath1*). Inactivation of *ATH1* in *pny pnf* rescues internode elongation and flowering. H, *knat6 pny pnf* mutant (similar to the wild type). Inactivation of *KNAT6* in *pny pnf* rescues internode elongation and flowering. I, *knat2 pny pnf* mutant (identical to *pny pnf* mutant). Bars = 2 cm.

induction by BOP1 may be direct. We tested this by analyzing *ATH1* and *KNAT6* expression in response to DEX induction in the presence of the protein synthesis inhibitor cycloheximide (CHX). After 2 and 4 h of combined treatment with DEX and CHX, *ATH1* transcripts were increased 5- to 7.5-fold relative to CHX-treated control plants. *KNAT6* transcripts were increased up to 2-fold after combined DEX and CHX treatment but not after DEX alone. Presumably, this is an indirect effect of BOP1 dependent on repression of protein synthesis. These data are consistent with *ATH1* being a direct target of BOP1 and *KNAT6* being an indirect target.

To examine tissue specificity of this interaction, 3.3- and 2-kb *ATH1p*:*GUS* reporter genes expressed in *D35S*:*BOP1-GR* ("Materials and Methods") were monitored for induction by DEX. Consistent with previous reports (Proveniers et al., 2007; Gómez-Mena and Sablowski, 2008), these reporters were expressed in shoot apices, leaves, and floral organ abscission zones and weakly expressed in the stem. After 4 h of DEX treatment, GUS activity was enhanced relative to mock-treated controls for both promoter lines in all tissues (Fig. 5, A–H). These data confirm that the *ATH1* promoter is responsive to BOP1 induction.

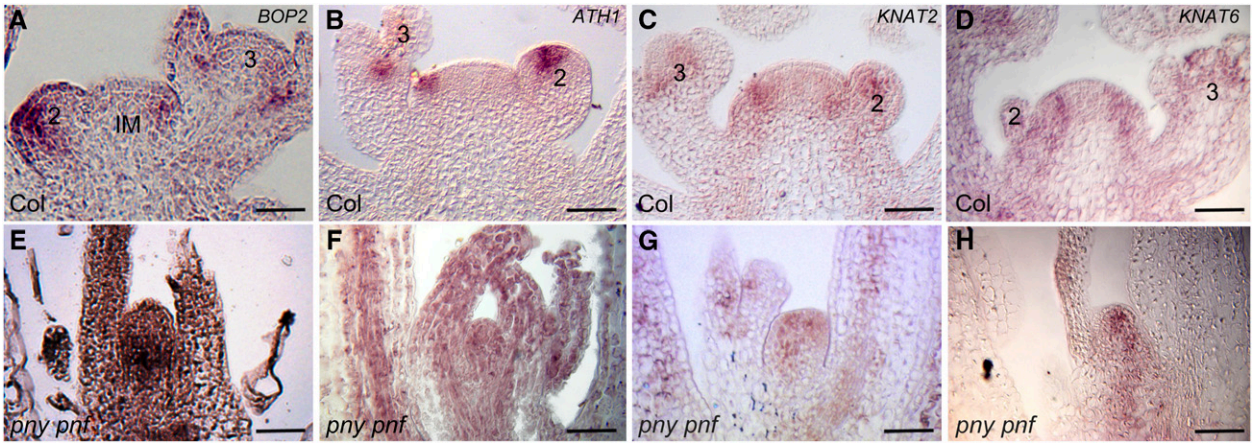

Figure 3. *BOP2*, *ATH1*, *KNAT2*, and *KNAT6* expression in *pny pnf* apices. Plants were grown for 3 weeks under SDs and transferred to continuous light to induce flowering. Apices were harvested on day 15. Transcript accumulation was monitored by in situ hybridization using longitudinal sections of Col-0 (A–D) and *pny pnf* (E–H) apices and gene-specific probes. Numbers in panels indicate the stage of floral development (Smyth et al., 1990). A, Col-0 apex showing *BOP2* expression in floral meristems (until stage 2) and the boundary domains of older flowers (late stage 2 and stage 3 are shown). B, Col-0 apex showing *ATH1* expression in an incipient floral primordium and the dome of a stage 2 flower. C, Col-0 apex showing *KNAT2* transcripts localized to boundary domains flanking the IM and older flowers. Expression is also observed in floral primordia and the dome of stage 2 flowers. D, Col-0 apex showing *KNAT6* transcripts localized to boundary domains flanking the IM and in a stage 3 flower. E to H, *pny pnf* apices showing expanded expression of *BOP2* (E), *ATH1* (F), *KNAT2* (G), and *KNAT6* (H) in the central and rib zones of the meristem. Bars = 40 μm.

BTB-ankyrin proteins, including BOP1/2, have no DNA-binding domain and interact with TGA bZIP binding factors for recruitment to DNA (Després et al., 2000; Hepworth et al., 2005; Xu et al., 2010; Khan et al., 2014). Direct association of BOP1 with the *ATH1* promoter was tested by chromatin immunoprecipitation (ChIP) using an anti-GR antibody followed by quantitative reverse transcription (qRT)-PCR. Leaf material was collected from *BOP1p*:*BOP1-GR bop1 bop2* flowering plants. Assays were performed using eight sets of primers spanning 2,178 bp of genomic sequence upstream of the *ATH1* transcription start site based on regions enriched in TGA bZIP binding sites (Fig. 5I; see "Materials and Methods"). Motifs that match or closely match consensus binding sites for TGA factors are also found in the intragenic and 3′ untranslated regions of the *ATH1* genomic sequence (data not shown). Quantitative analysis by qRT-PCR revealed at least one position in the *ATH1* promoter (site IV) showing a reproducible 1.77-fold enrichment of BOP1 protein in DEX-treated plants (Fig. 5J). ChIP assays performed using the mock control showed no significant enrichment at this position or the control *UBIQUITIN5* (*UBQ5*) genomic region. Site IV (nucleotides −2,686 to −2,577) is located approximately 1,515 bp upstream of the *ATH1* transcription start site and found within the 3.3-kb *ATH1p*:*GUS* construct that is responsive to BOP1 induction in leaves and inflorescences (Fig. 5). Site VII (nucleotides −1,529 to −1,416) was identified as a second potential binding site. Taken together, these data support that BOP1 directly associates with the *ATH1* promoter in vivo to regulate its transcription.

Restored Accumulation of Flowering Transcripts in *pny pnf* Apices after Rescue by Inactivation of *BOP1/2*, *KNAT6*, and *ATH1*

Nonflowering *pny pnf* apices accumulate *SOC1* and *FUL* transcripts markers of inflorescence identity but fail to accumulate *FT* or *LFY*, *AP1*, and *CAL* markers of floral fate (Smith et al., 2004; Kanrar et al., 2008). Accumulation of *SPL3*, *SPL4*, and *SPL5* transcripts is also diminished in *pny pnf* apices (Lal et al., 2011). Flowering time of wild-type plants was compared with those of *bop1 bop2 pny pnf*, *knat6 pny pnf*, and *ath1 pny pnf* mutants to further quantify rescue. Figure 6A shows that flowering time for *knat6 pny pnf* mutants and wild-type control plants was similar. Flowering time of *bop1 bop1 pny pnf* mutants was slightly delayed (+3.6 d) and flowering time of *ath1 pny pnf* mutants was slightly earlier (−6.9 d) than the wild type, consistent with parental controls (Fig. 6A; Xu et al., 2010). To test if inactivation of *BOP1/2*, *ATH1*, and *KNAT6* correlates with restored expression of meristem identity genes in *pny pnf* apices, we measured relative transcript abundance in the wild type and mutants; 25-d-old plants grown under SDs were transferred to LDs to induce flowering. Apices were harvested 12 d later. The floral transition was complete for all genotypes at this time point. Figure 6B confirms that *SOC1* and *FUL* transcripts are relatively unchanged in the wild type compared with mutants. Figure 6B also shows that low to undetectable levels of *FD*, *LFY*, *AP1*, and *CAL* transcripts in *pny pnf* apices resumed expression in triple and quadruple mutants, except for *CAL*, which remained low in *bop1 bop2 pny pnf* apices. Transcripts for *FUL*, *LFY*, *AP1*, and

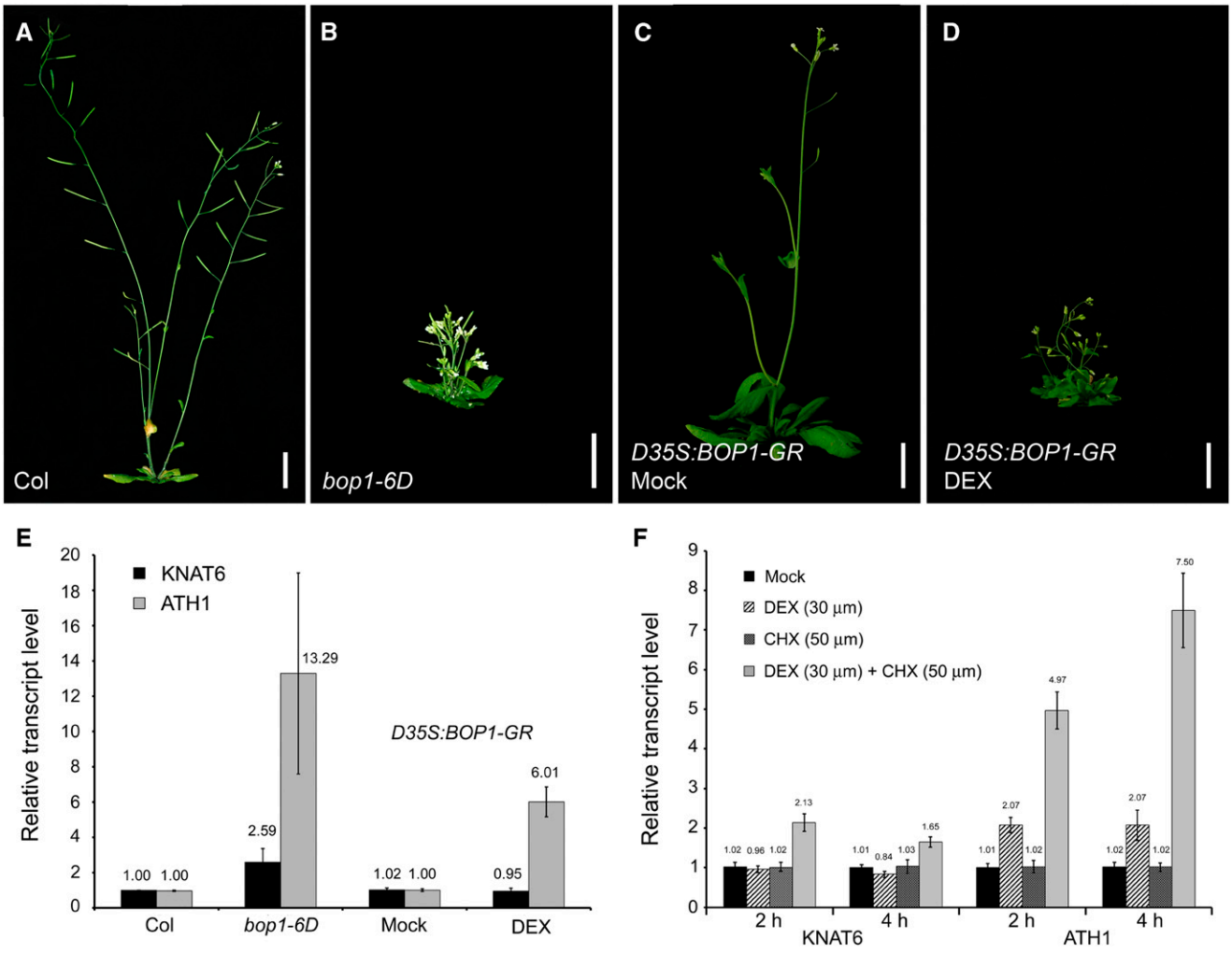

Figure 4. Activation of *ATH1* and *KNAT6* in the DEX-induced *D35S:BOP1-GR* line. A, Col-0 plant. B, *bop1-6D* mutant with shortened internodes and clustered siliques. C and D, *D35S:BOP1-GR* plants treated with mock or DEX solutions for 4 weeks. C, Mock-treated *D35S:BOP1-GR* plant showing a wild-type phenotype. D, DEX-induced *D35S:BOP1-GR* plant showing a phenotype similar to *bop1-6D* mutant. E, Comparison of *KNAT6* and *ATH1* transcript levels in the wild type versus *bop1-6D* mutants and mock- versus DEX-induced *D35S:BOP1-GR* plants after continuous treatment for 4 weeks. F, Comparison of *KNAT6* and *ATH1* transcript levels in DEX-induced *D35S:BOP1-GR* lines with and without protein synthesis inhibitor CHX. Transcripts were measured after 2 and 4 h of treatment. Bars = 2 cm.

CAL were elevated in *ath1 pny pnf* apices, consistent with earlier flowering. Figure 6C shows that patterns of *miR156* and *SPL* transcript accumulation in triple and quadruple mutants are likewise restored to resemble the wild type. Collectively, these data show that PNY-PNF is dispensable for flowering when BOP1/2, ATH1, and KNAT6 activities are eliminated.

BOP1 Overexpression Mimics *pny pnf* Defects in *SPL* Transcript Accumulation and Responsiveness to GA

Given that *pny pnf* mutants misexpress *BOP1/2*, we used transcript profiling to test if dwarfism and late flowering exhibited by the gain-of-function *bop1-6D* mutant impact similar pathways. We first monitored the accumulation of *miR156* and *SPL* transcripts in *bop1-6D* internodes for comparison with *pny pnf* using qRT-PCR (Fig. 7A). These data show that *miR156* transcripts in *bop1-6D* are 1.4-fold up-regulated relative to the wild type. In addition, *SPL* transcripts in *bop1-6D* were significantly down-regulated, with the exception of *SPL5*. These data suggest that *bop1-6D* partially mimics *pny pnf* (compare Fig. 6C with Fig. 7A).

To further explore similarities and differences between these two mutants, we examined transcripts involved in the regulation of GA, which is a positive regulator of internode elongation and flowering (Mutasa-Göttgens and Hedden, 2009; Porri et al., 2012). The expression levels of genes required for GA biosynthesis and catabolism and DELLA repressors of GA signaling were monitored by qRT-PCR in *pny pnf* apices

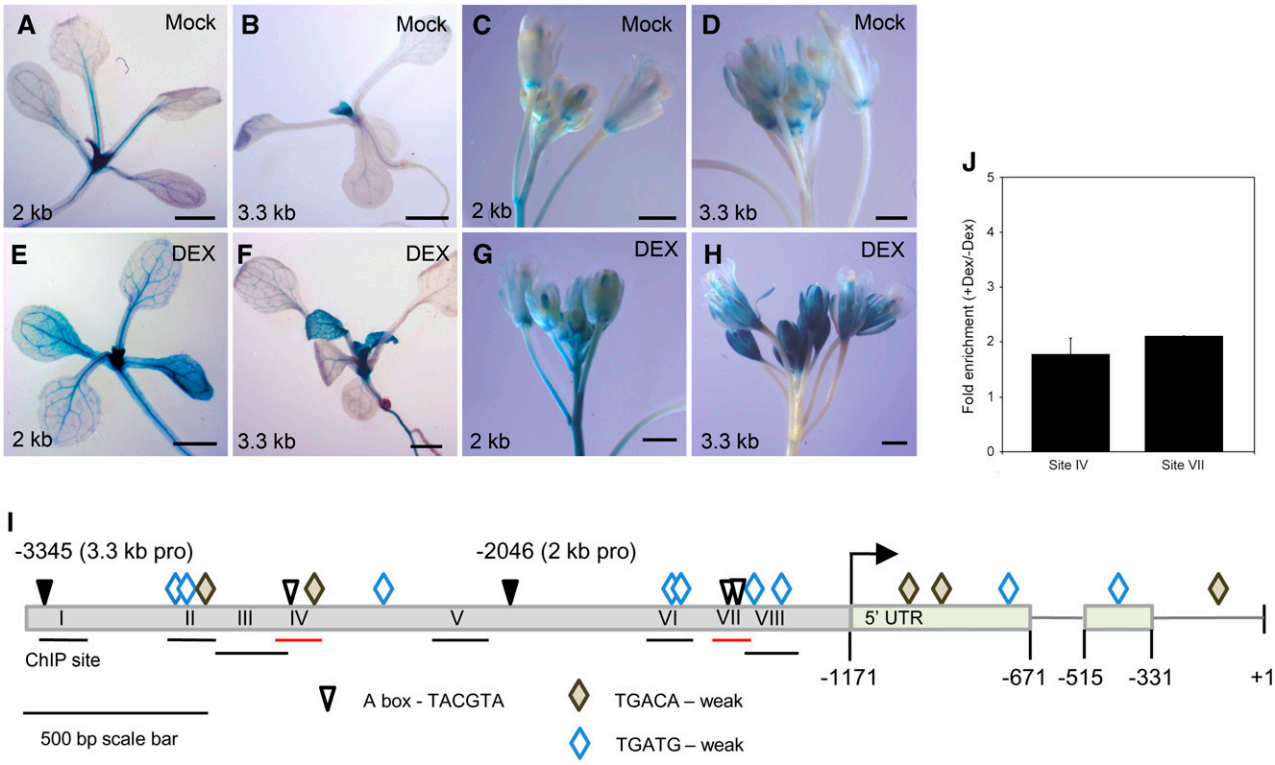

Figure 5. Identification of the genomic region responsible for *ATH1* induction by BOP1. A to H, Functional characterization of the *ATH1* regulatory region. Representative expression patterns are shown for *D35S:BOP1-GR* plants containing 2- (A, C, E, and G) or 3.3-kb (B, D, F, and H) *ATH1p:GUS* reporter genes as diagrammed in I. Promoter activity was monitored by GUS staining after incubation of 10-d-old seedlings or 6-week-old inflorescences for 4 h in mock or 30 μm of DEX solution. Comparison of mock (A–D) and DEX (E–H) shows that expression is up-regulated in the leaves, flowers, and stem of DEX-induced lines for both promoter constructs. Bars = 1 mm. I, Map of the *ATH1* promoter and 5′ untranslated region. Black arrowheads mark the 5′ ends of genomic fragments used in construction of 2- and 3.3-kb *ATH1p:GUS* reporter genes. Predicted consensus binding sites for TGA bZIP factors (Schindler et al., 1992; Izawa et al., 1993; Fode et al., 2008) are shown in relation to fragments amplified by qRT-PCR after ChIP to test for BOP1 localization (horizontal bars). Sites in red (IV and VII) contain A boxes and show enrichment for BOP1. J, Quantification of BOP1-GR enrichment at sites IV and VII in the *ATH1* promoter by qRT-PCR. Anti-GR ChIP was performed using leaves from mock- and DEX-treated *35S:BOP1-GR bop1 bop2* plants. Fold enrichment at sites IV and VII is presented as the ratio of DEX versus mock transcript levels after normalization to the unrelated *UBQ5* control sequence. Three biological replicates were quantified to show enrichment at site IV. One biological replicate was quantified to show enrichment at site VII. Three technical replicates were performed for each. Error bars indicate SD.

and *bop1-6D* apices and internodes and revealed similar patterns (Fig. 7, B–D). In both genotypes, there was little or no change in *ent*-kaurene synthase (KS) transcript, but *GA20ox1* transcripts were significantly increased (Fig. 7, C and D; Yamaguchi, 2008). In *bop1-6D*, there was a compensatory decrease in *GA3ox1* transcripts functioning later in the biosynthetic pathway (Fig. 7D; Yamaguchi, 2008). In internodes, there was also a compensatory increase in *GA2ox7* transcripts required in catabolism (Fig. 7, B and D; Yamaguchi, 2008). All five *DELLA*s encoding repressors of GA signaling were up-regulated in *pny pnf*, whereas selective up-regulation of *REPRESSOR OF GA1-3 LIKE3* (*RGL3*) was observed in *bop1-6D* (Fig. 7, C and D). These data indicate that GA homeostasis is disrupted in both mutants. Nevertheless, deficiency alone does not account for phenotypic defects. Spray treatments with GA_3 failed to rescue flowering in *pny* and did not enhance internode elongation in *bop1-6D*, although this mutant flowered 4 d earlier than mock-treated control plants (Fig. 7, E and F; Smith et al., 2004). In conclusion, *SPL* transcript accumulation and responsiveness to GA are blocked in both mutants. We, therefore, used microarray analysis of *bop1-6D* internodes to identify additional factors that might antagonize flowering and internode elongation in these mutants.

Overexpression of *BOP1* Activates Stress Pathways and Promotes Accumulation of JA as a Mechanism for Repression of Growth and Flowering

The transcriptomes of *bop1-6D* versus wild-type internodes were assessed by microarray ("Materials and Methods"). Gene Ontology (GO) analysis of differentially regulated genes revealed significant enrichment

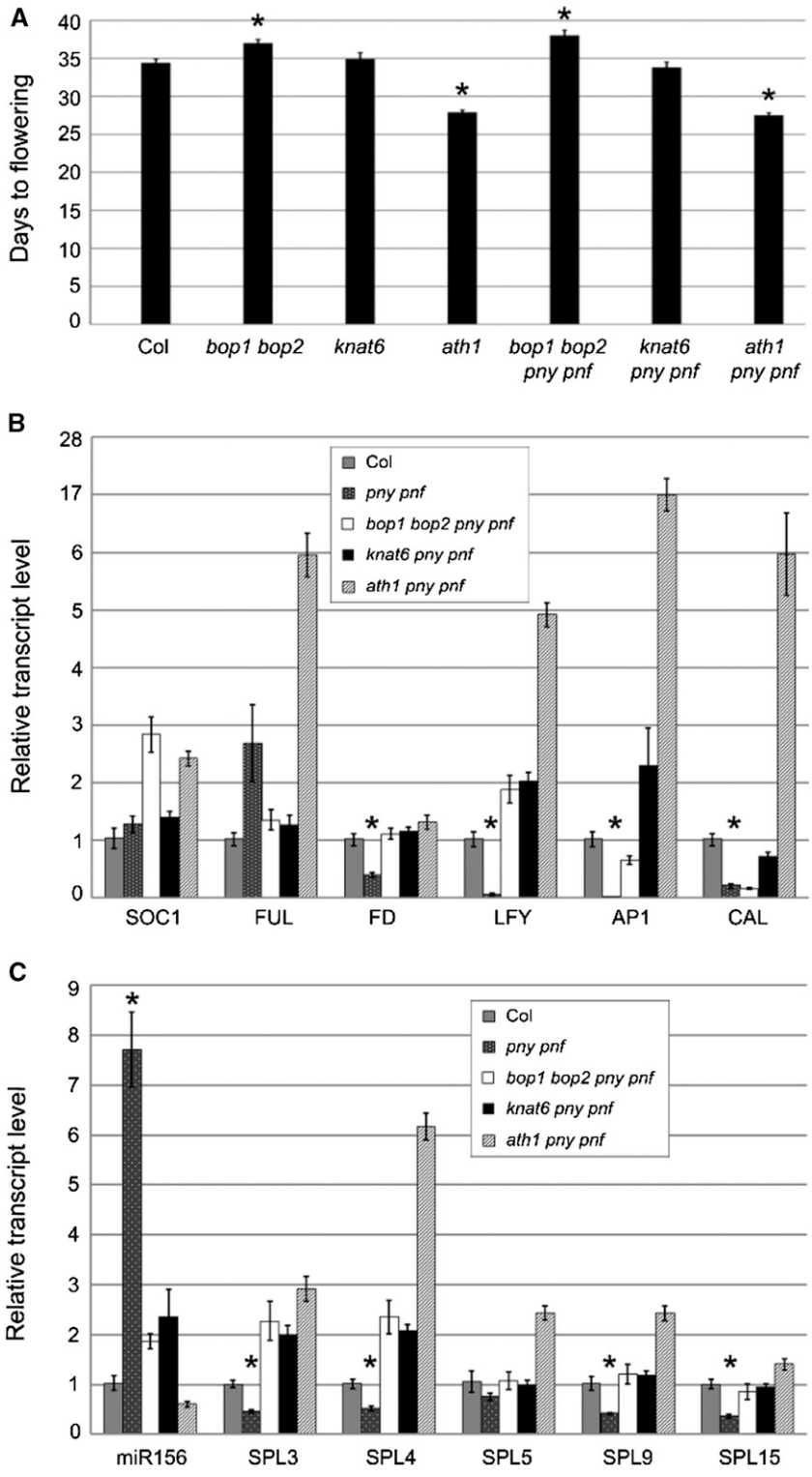

Figure 6. Quantification of flowering time and meristem identity transcripts in the wild type and mutants. A, Quantitative analysis of flowering time. Plants were grown under LDs. Date of apex emergence for *bop1 bop2 pny pnf*, *knat6 pny pnf*, and *ath1 pny pnf* mutants is comparable with that of the wild type with minor variations. Lines containing *ath1* flowered slightly earlier (−6.7 d) and lines containing *bop1 bop2* flowered slightly later (+3.1 d) than the wild type. *, Significant differences (Student's *t* test; $P < 0.01$). B, Quantitative analysis of meristem identity gene expression. Flowering was induced by shifting plants from SDs to LDs. Apices were harvested on day 37 at the end of 12 LDs. IM identity gene transcripts *SOC1* and *FUL* are expressed at similar levels in Col-0 and *pny pnf* apices. Floral meristem identity gene transcripts *FD*, *LFY*, *AP1*, and *CAL* are significantly lower in *pny pnf* compared with Col-0 apices. Transcript accumulation resumes in *bop1 bop2 pny pnf*, *knat6 pny pnf*, and *ath1 pny pnf* apices. *, Significant differences (Student's *t* test; $P < 0.05$). C, Quantitative analysis of *miR156* and *SPL* transcript abundance in wild-type and mutant apices. Nonflowering in *pny pnf* correlates with a significant increase in *miR156* abundance at the expense of *SPL3*, *SPL4*, *SPL6*, *SPL9*, and *SPL15* transcripts relative to Col-0 plants. Transcript accumulation in *bop1 bop2 pny pnf*, *knat6 pny pnf*, and *ath1 pny pnf* mutants follows a pattern similar to the wild type, consistent with restored flowering. *, Significant differences (Student's *t* test; $P < 0.05$).

of terms associated with response to biotic and abiotic stress stimuli (Supplemental Table S1). Response to JA stimulus (GO:009753) was at the top of the list, but other hormone pathways associated with stress showed similar enrichment. In descending order, these were response to salicylic acid stimulus (GO:0009751), response to ethylene stimulus (GO:009723), and response to abscisic acid stimulus (GO:0099737). These data suggest that *bop1-6D* plants have heighted expression of stress-related genes. Trade-offs between plant defense and plant growth are well established in the recent literature (Navarro et al., 2008; Wild et al.,

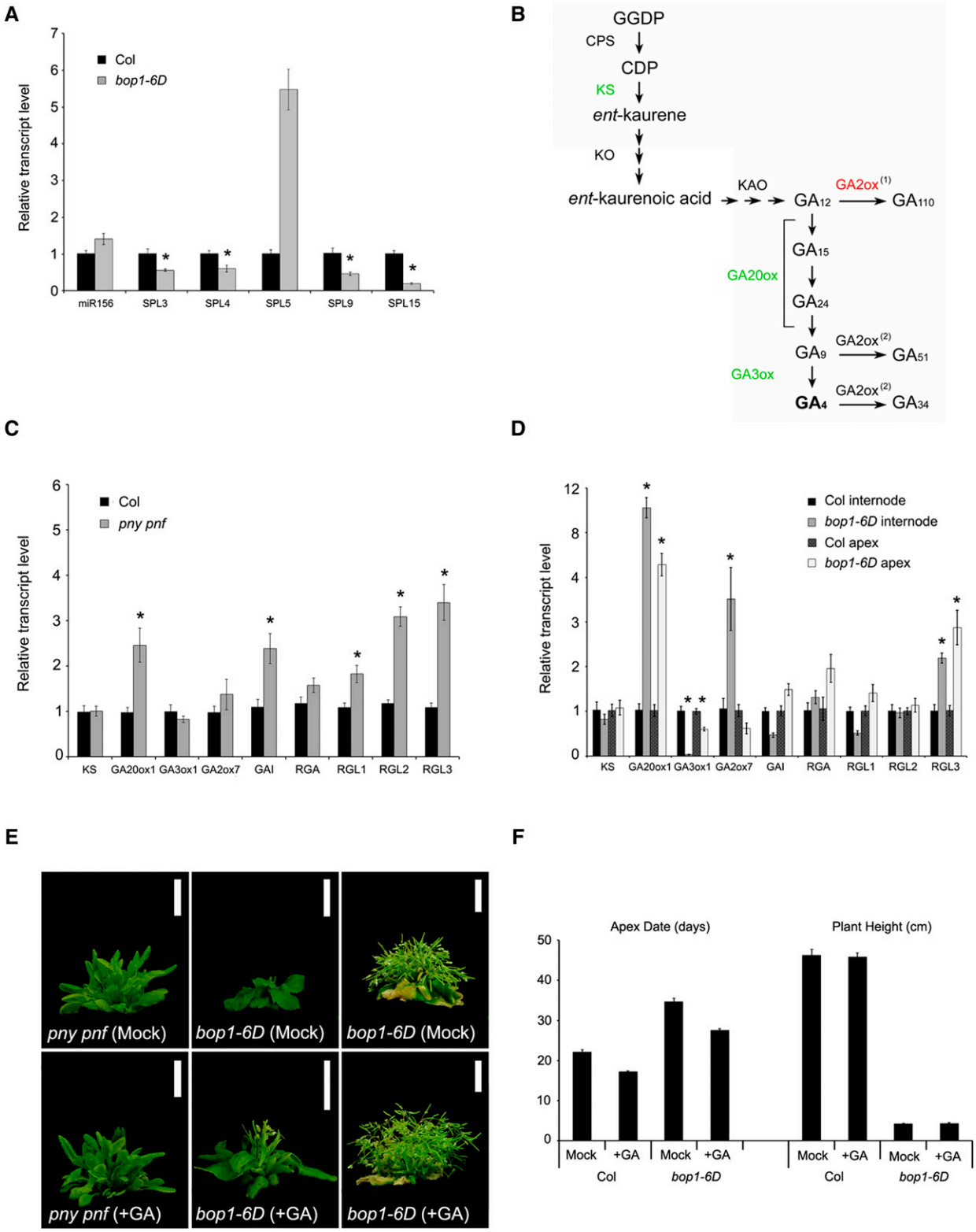

Figure 7. *BOP1* overexpression mimics *pny pnf* defects in *SPL* transcript accumulation and GA homeostasis. Plants were grown in continuous light. qRT-PCR was used to assess transcript accumulation in apices and/or internodes. A, Accumulation of *miR156* and *SPL* transcripts in Col-0 and *bop1-6D* internodes. B, Schematic representation of non-13-hydroxylated GA biosynthetic and catabolic pathways in Arabidopsis (Hu et al., 2008; Yamaguchi, 2008). Green lettering indicates GA biosynthetic enzymes monitored for transcript accumulation in C and D. Red lettering indicates GA catabolic enzyme monitored for transcript accumulation in C and D. Bioactive GA_4

2012; Yang et al., 2012; Wild and Achard, 2013), and therefore, we further explored this mechanism. We specifically examined floral repressors in the microarray using a candidate gene approach (Fig. 8A). This analysis revealed up-regulation of DELLA, FLOWERING LOCUS C (FLC)-LIKE (FLC-like), and AP2-like members. However, the highest fold changes were observed among AP2/ETHYLENE RESPONSE FACTOR (ERF)-like factors that repress growth and flowering under stress conditions (Magome et al., 2004, 2008; Kang et al., 2011; for review, see Licausi et al., 2013). To validate these findings, selected transcripts were quantified by qRT-PCR using independently isolated tissue samples. Floral repressor transcript profiles of *bop1-6D* and *pny pnf* apices genotypes showed strong agreement (Fig. 8B). Consistent with the microarray, no significant change was observed for *FLC*, but transcripts encoding AP2-like repressors TARGET OF EAT2 (TOE2; 1.6- to 4-fold) and SCHLAFMUTZE (SMZ; 8.5- to 21-fold) were highly up-regulated compared with the wild type. The highest fold changes (6.2- to 454-fold) were observed for stress-induced AP2/ERF floral repressor transcripts, including *DWARF AND DELAYED FLOWERING1* (*DDF1*) and *DDF2*, which encode proteins that inhibit growth by reducing bioactive GA content (Magome et al., 2004, 2008; Kang et al., 2011; for review, see Licausi et al., 2013).

Inspection of the microarray also showed an increase in expression of biosynthetic enzymes for JA (Fig. 9, A and B). Validation of these data by qRT-PCR confirmed significant up-regulation of transcripts involved in JA biosynthesis in *bop1-6D* and *pny pnf* tissues (Fig. 9C). To determine if these increases reflect changes in hormone accumulation in plants, JA levels were quantified in internodes and buds from *bop1-6D* and *pny pnf* apices ("Materials and Methods"). BOP1-overexpressing plants showed 2.5-fold higher levels of JA relative to wild-type plants (Fig. 9D). Conversely, hormone levels were decreased in *bop1 bop2* compared with wild-type control plants. *pny pnf* apices showed 1.5-fold higher levels of JA relative to wild-type control apices at the same stage of development (Fig. 9D). These data suggest that BOP1/2 promotes JA production.

To further examine JA effects on reproductive plant development, methyl jasmonate (MeJA) was applied to wild-type and *pny* plants grown under LDs (Fig. 10). Plants of both genotypes treated with MeJA developed a compact rosette with small dark green leaves, similar to those of *bop1-6D* mutants (Fig. 10, A–C). Wild-type plants treated with MeJA showed partial loss of apical dominance similar to *pny* mutants (Fig. 10, D–G). Plants in both treatment populations were late flowering with short internodes relative to mock-treated control plants (Fig. 10, D–G) and similar to *pny pnf*/+ mutants (Supplemental Fig. S1, A–G). Organ fusions or clusters were not observed. In both wild-type and *pny* populations, a small subset of plants developed a disordered rosette phenotype similar to *pny pnf* mutants and were nonflowering after 10 weeks (data not shown). No such defects were observed in mock-treated control plants. Thus, treatment of wild-type plants with exogenous MeJA mimics the phenotype of *bop1-6D* and *pny* or *pny pnf*/+ plants.

In parallel, we tested if reducing JA content rescues internode elongation or flowering in *pny pnf* and/or *bop1-6D* mutants by crossing them to the *allene oxide synthase* (*aos*) mutant, which is defective JA synthesis (Park et al., 2002; Figs. 7B and 10). Triple mutants with *pny pnf* remained nonflowering, even with addition of exogenous GA_3 (Fig. 10H; data not shown). However, quantitative analysis of *bop1-6D aos* double mutants revealed a small but significant ($P \leq 0.0001$) increase in flowering time (+1.8 d) and plant height (+1.5 cm) compared with *bop1-6D* siblings in a segregating population (Fig. 10, I and J). These data provide evidence that modulation of growth by JA is a potential factor in conditioning *bop1-6D* and *pny pnf* phenotypic defects.

DISCUSSION

Floral evocation is dependent on SAM restructuring to form an IM (Bernier, 1988). The TALE homeodomain PNY and PNF transcription factors are essential for this process by permitting responsiveness to floral inductive signals (Smith et al., 2004; Kanrar et al., 2008; Lal et al., 2011; Smith et al., 2011; Ung et al., 2011; Ung and Smith, 2011). In *pny pnf* mutants, meristems support the production of leaves, but internode elongation and flower initiation are blocked.

In this article, we characterized the interaction of PNY and PNF with lateral organ boundary factor BOP1/2 and a pair of downstream effectors: the KNOX-BELL homeodomain factors KNAT6 and ATH1. We show that misexpression of these genes in *pny pnf* apices blocks floral evocation (Fig. 11). Inactivation of *BOP1/2* and *ATH1* or *KNAT6* fully restores *pny pnf* defects in meristem and boundary maintenance and stem elongation and restores expression of floral meristem identity genes to allow flowering. Remarkably, other factors compensate for the loss of these genes in maintaining the SAM and responsiveness to floral inductive signals. Thus, PNY and PNF allow flowering by excluding boundary genes from the meristem. Similar antagonistic interactions for PNY or BP with members of the BOP1/2-ATH1/KNAT6 module

Figure 7. (*Continued.*)
is indicated in bold. Inactive GA metabolites shown on right. CDP, *ent*-Copalyl diphosphate; CPS, *ent*-copalyl diphosphate synthase; GGDP, geranylgeranyl diphosphate; KAO, *ent*-kaurenoic acid oxidase; KO, *ent*-kaurene oxidase; KS, *ent*-kaurene synthase. C and D, Accumulation of GA pathway transcripts in *pny pnf* apices and *bop1-6D* apices and internodes. E, *pny pnf* and *bop1-6D* plants treated with 100 μm of GA_3 or a mock solution. F, Flowering time and plant height of Col-0 and *bop1-6D* plants treated with 100 μm of GA_3 or a mock solution. *, Significant differences (Student's *t* test; $P < 0.05$).

A

Repressor	Gene Name	Log_2FC
DELLA		
At5g17490	*RGL3*	1.20
FLC-clade		
At1g77080	*MAF1 (AGL27)*	0.64
At5g65060	*MAF3 (AGL70)*	0.50
At5g65080	*MAF5 (AGL68)*	1.26
AP2-like		
At5g60120	*TOE2*	0.56
At3g54990	*SMZ*	0.80
AP2/ERF		
At1g12610	*DDF1*	3.22
At1g63030	*DDF2*	0.89
At4g25470	*CBF2*	1.25
At5g51990	*CBF4*	1.31
At1g12610	*TINY2*	0.55

B

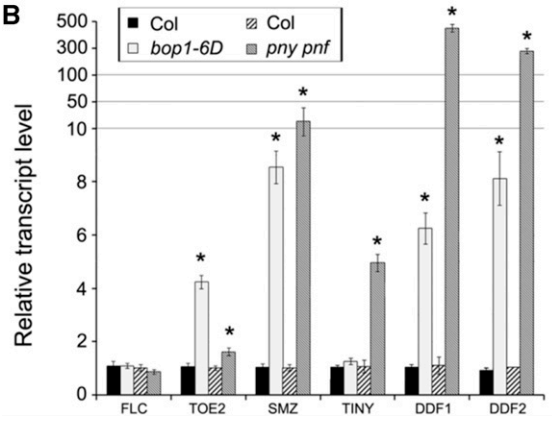

Figure 8. Transcript profiling of floral repressor genes in *bop1-6D* and *pny pnf* mutants. A, Floral repressor genes differentially expressed in *bop1-6D* compared with Col-0 internodes according to microarray experiment ("Materials and Methods"). B, Repressor transcript profile of *bop1-6D* and *pny pny* mutants quantified by qRT-PCR. No differential expression was observed for *FLC* transcript. Transcripts encoding AP2-like TOE2 and SMZ repressors and AP2/ERF Dehydration-responsive Element (DRE)-binding Protein-like TINY, DDF1, and DDF2 repressors were differentially up-regulated in agreement with A. *, Significant differences (Student's *t* test; $P < 0.05$).

function in various other developmental contexts, including abscission, fruit patterning, and inflorescence architecture (Ragni et al., 2008; Shi et al., 2011; Khan et al., 2012a, 2012b; Li et al., 2012).

We further investigated the organization of this module and its transcriptional targets. Our data show that BOP1 is a direct regulator of *ATH1*, whereas promotion of *KNAT6* is probably indirect. Indeed, DEX and CHX treatment of *35S:ATH1-GR* plants produces rapid induction of *KNAT6* transcript, and reporter gene expression is missing at boundaries in *ath1-3* but not *bop1 bop2* mutants, suggesting a direct requirement for ATH1 (data not shown). BOP1/2 coactivators are recruited to DNA through interactions with TGA bZIP transcription factors (Hepworth et al., 2005; Xu et al., 2010). These TGA factors remain unknown in the context of flowering, but several candidates are being investigated (Fig. 11). Transcript profiling was used to probe how this module blocks flowering. Comparison of the gain-of-function *bop1-6D* mutant and *pny pnf* showed similar transcriptional defects in core pathways controlling flowering. Our data are consistent with the model that BOP1/2-ATH1/KNAT6 boundary genes activate stress pathways that promote JA biosynthesis, which directly or indirectly interferes with signals integrated by the *miR156-SPL-miR172* module to antagonize IM function (Fig. 11). Details of this model are discussed below.

The *miR156-SPL-miR172* Module as a Hub for Integration of Flowering Signals

The *miR156-SPL-miR172* module is a core pathway for integration of flowering signals, including age, sugar, GA, and stress (Huijser and Schmid, 2011; Cho et al., 2012; Proveniers, 2013; Cui et al., 2014; Stief et al., 2014; Wang, 2014). In brief, *miR156* levels decline with age, leading to a concomitant increase in abundance of *SPL* transcripts with products that act on distinct targets in leaves and the shoot apex to promote flowering (Wu and Poethig, 2006; Wang et al., 2009; Wu et al., 2009). SPL3 and SPL9 members in the SAM directly promote the activation of floral meristem identity genes (Wu et al., 2009; Yamaguchi et al., 2009). SPL9-like members have additional functions in leaves, where they activate the transcription of *miR172b*, which lowers the abundance AP2-like floral repressor transcripts and allows accumulation of *FT* mRNA (Zhu and Helliwell, 2011; Matsoukas et al., 2012; Wang, 2014).

Significant reduction of *miR156*-regulated *SPL* transcripts was observed in *pny pnf* and *bop1-6D* mutants. This reduction is likely driven by multiple factors, including lower levels of FD, which recruits FT to the promoter of *SPL*s for activation (Jung et al., 2012; Andrés et al., 2015), and higher steady-state levels of *miR156* (Lal et al., 2011). An increase in *miR156* was less marked in *bop1-6D*, suggesting that the reduction in *SPL* transcript is mediated by *miR156* and other regulators. These data are consistent with previous work showing that *SPL3/4/5* transcripts are reduced in *pny pnf* apices and partly account for nonflowering (Lal et al., 2011). Transgenic *pny pnf* plants expressing an *miR156*-resistant form of *SPL4* were restored for *LFY* and *AP1* expression but only partly restored for flowering, suggesting that multiple *SPL* factors are involved (Lal et al., 2011).

Concomitantly, transcripts encoding *miR172*-regulated AP2-like repressors of flowering and internode elongation were elevated in *bop1-6D* and *pny pnf* mutants. This group of repressors includes AP2, SMZ, TOE1, TOE2, and

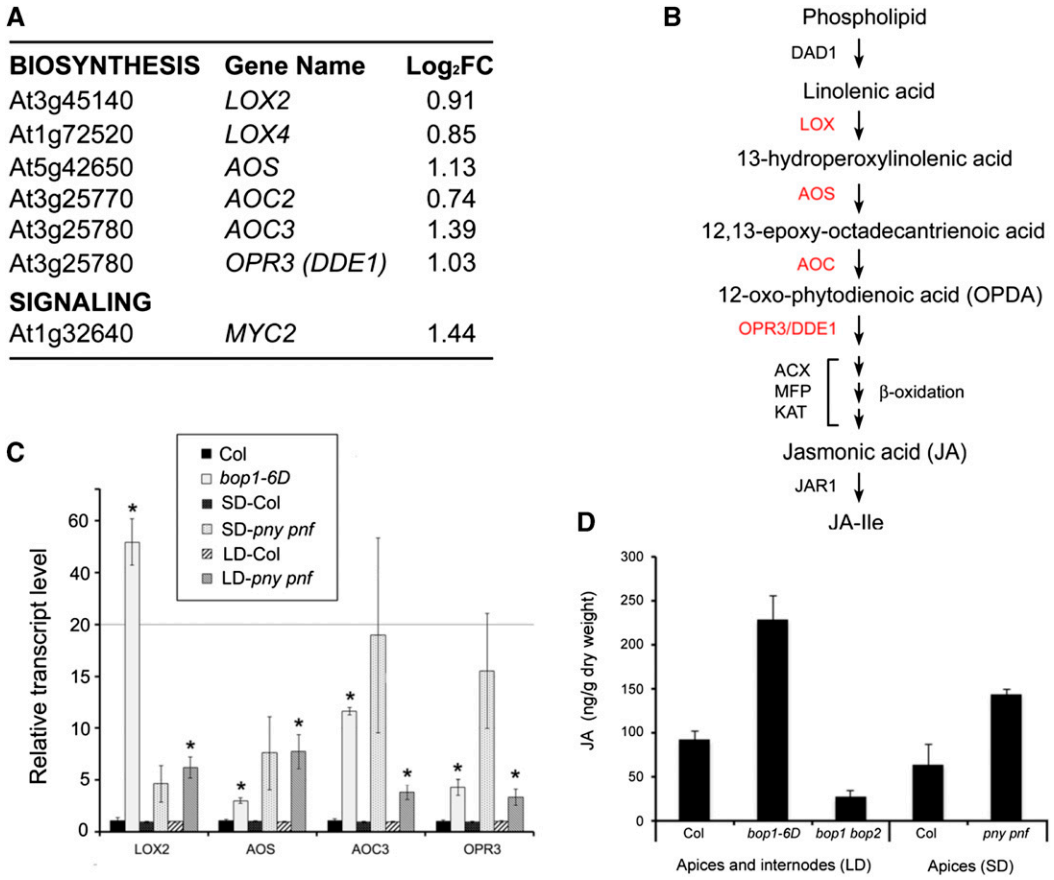

Figure 9. *BOP1* overexpression increases JA content by transcriptional up-regulation of biosynthetic genes. A, JA-related genes differentially expressed in *bop1-6D* compared with Col-0 internodes identified by microarray experiment ("Materials and Methods"). B, Schematic representation of the JA biosynthetic pathway in Arabidopsis (Park et al., 2002; Wasternack and Hause, 2013). Red lettering indicates transcripts investigated by qRT-PCR in C. Linolenic acid is released from membrane lipids by a lipolytic enzyme (DEFECTIVE IN ANTHER DEHISCENCE1 [DAD1]) and converted to allene oxide (12,13-epoxy-octadecantrienoic acid) by lipoxygenase (LOX) and AOS. One cyclization, one reduction, and three rounds of β-oxidation steps are required in producing JA, which is conjugated to Ile (JA-Ile) in bioactive form (Wasternack and Kombrink, 2010). ACX, Acetyl-CoA oxidase; AOC, allene oxide cyclase; JAR1, JASMONATE RESISTANT1; KAT, L-3-ketoacyl CoA thiolase; MFP, multifunctional protein; OPR3/DDE1, 12-oxo-phytodienoic acid-10,11-reductase3/DELAYED DEHISCENCE1. C, Quantitative analysis of JA biosynthetic gene transcripts in *bop1-6D* and *pny pnf* mutants grown under SDs or LDs. *, Significant differences (Student's *t* test; $P < 0.05$). D, Concentration of JA in wild-type tissues compared with *bop1-6D*, *bop1 bop2*, and *pny pnf* mutants ("Materials and Methods").

TOE3 with overlapping functions (Aukerman and Sakai, 2003; Jung et al., 2007; Mathieu et al., 2009; Yant et al., 2010). SMZ and presumably, other members of this family delay flowering through the direct repression of *FT* and promotion of *miR156* (Mathieu et al., 2009; Yant et al., 2010). Of these, *TOE2* and *SMZ* show consistent up-regulation in the transcriptome of *bop1-6D* and *pny pnf* apices. Thus, overexpression of AP2-like members in *bop1-6D* may be a route to restricting internode elongation and flowering.

Integration with Signals for Stress and Carbohydrate Metabolism

Stress and sugar signals are also integrated through the *miR156-SPL-miR172* module to control flowering (for review, see Wang, 2014). Recent studies address the mechanism. One study shows that *miR156-SPL3* delays flowering under cool ambient temperatures by regulation of *FT* (Kim et al., 2012). Similarly, plants overexpressing *miR156* are late flowering with increased tolerance to stress linked to down-regulation of *SPL9* (Cui et al., 2014). Stief et al. (2014) further showed that heat stress induces *miR156* isoforms linked to down-regulation of *SPL9*-like transcripts (*SPL2*, *SPL9*, and *SPL11*) and delayed flowering. Induction of *miR156h* in this cascade is predicted to target the pectin methylesterase inhibitor *At5g38610* , which may affect bolting (Stief et al., 2014). PNY controls inflorescence patterning by regulating cell wall modification enzymes, including pectin methylesterases, which loosen cell walls in the stem to promote internode elongation and in the SAM to facilitate organ initiation (Etchells et al., 2012;

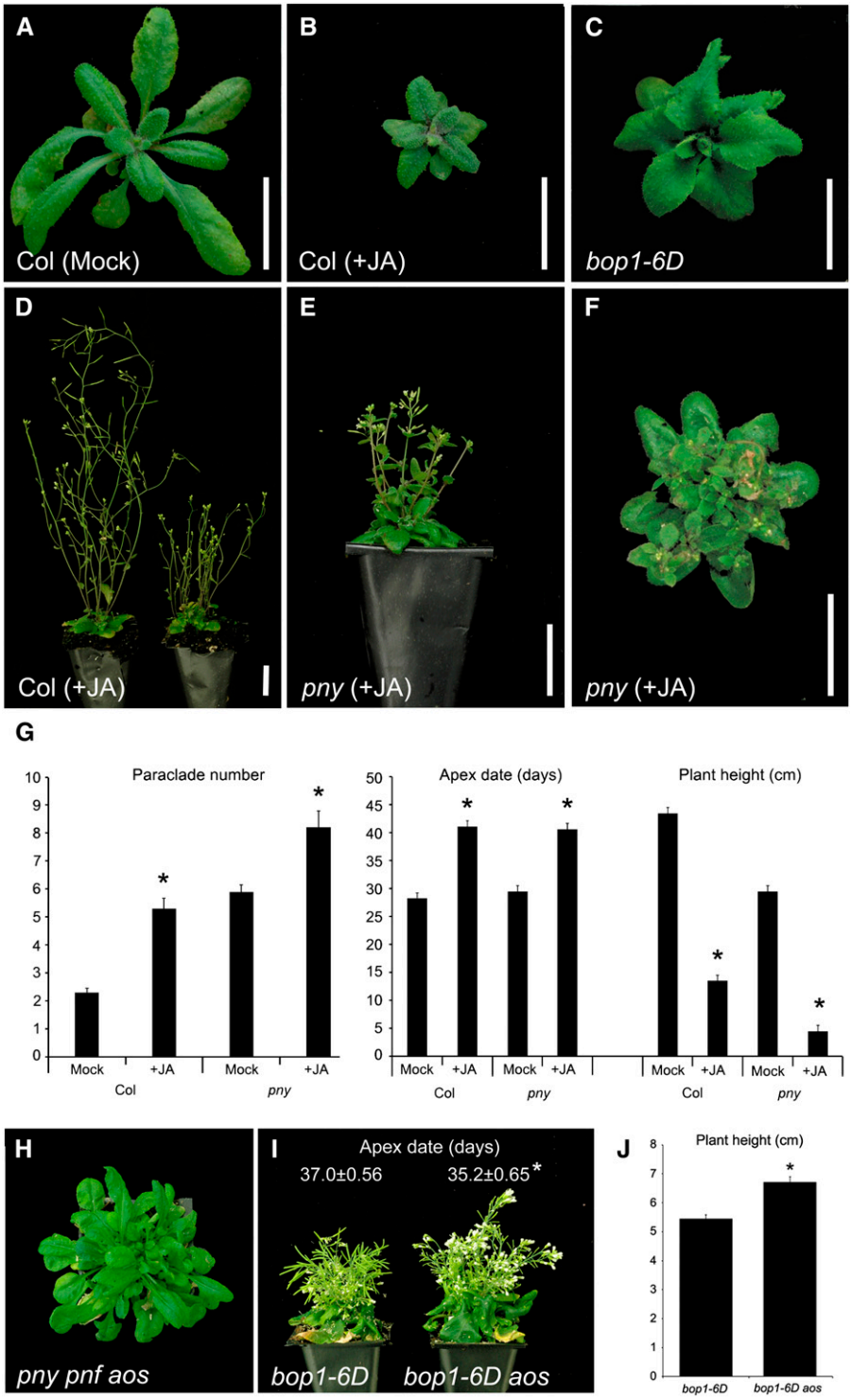

Figure 10. Effect of loss or gain of JA content on phenotype of the wild type and mutants. A to G, Wild-type and *pny* plants were sprayed daily until maturity with 100 μm of MeJA or a mock solution. A, Mock-treated Col-0 plant. B, MeJA-treated Col-0 plant showing small dark green leaves. C, *bop1-6D* mutant showing a compact rosette similar to that in B. D, JA-treated Col-0 plants showing *pny*-like partial loss of apical dominance and short stature. E, JA-treated *pny* mutant showing enhancement of defects in internode elongation and apical dominance relative to mock control (see G). F, JA-treated *pny* mutant showing delayed flowering relative to mock control. G, Quantitative phenotypic analysis of wild-type and *pny* mutant plants treated with MeJA. Plants were grown under LDs. For both genotypes, treatment with MeJA resulted in additional rosette paraclades, indicating loss of apical dominance, reduced height, and delayed flowering. H to J, Effect of *aos* loss of function on *pny pnf* and *bop1-6D* phenotypes. Representative plants are shown. H, *pny pnf aos* mutant remains nonflowering. I and J, Phenotype of *bop1-6D* versus *bop1-6D aos* mutants. A small but highly significant ($P <$ 0.0001) increase in plant height (+1.26 cm) and earlier flowering (−1.8 d) are measured in *bop1-6D aos* compared with *bop1-6D* control plants. Analysis was performed in a *bop1-6D/+ aos/+* segregating population ($n =$ 100). Bars = 1.5 cm. *, Significant differences (Student's *t* test; $P<0.05$).

Peaucelle et al., 2011). *At5g38610* and related genes are up-regulated in the transcriptome of *bop1-6D* internodes, whereas PNY-regulated *PECTIN METHYLESTERASE5* is down-regulated, consistent with dwarf stature (data not shown; Peaucelle et al., 2011).

The *miR156-SPL-miR172* module is also a sensor for nutrients. A developmental decline in *miR156* is partially mediated by sugars produced by photosynthesis that accumulate with age (Proveniers, 2013; Yang et al., 2013; Yu et al., 2013). Global transcript changes in *bop1-6D* mutants are characterized in large part by alterations in stress signaling and carbohydrate metabolism (Supplemental Table S1). GO enrichment analysis of the *bop1-6D* transcriptome identifies significant

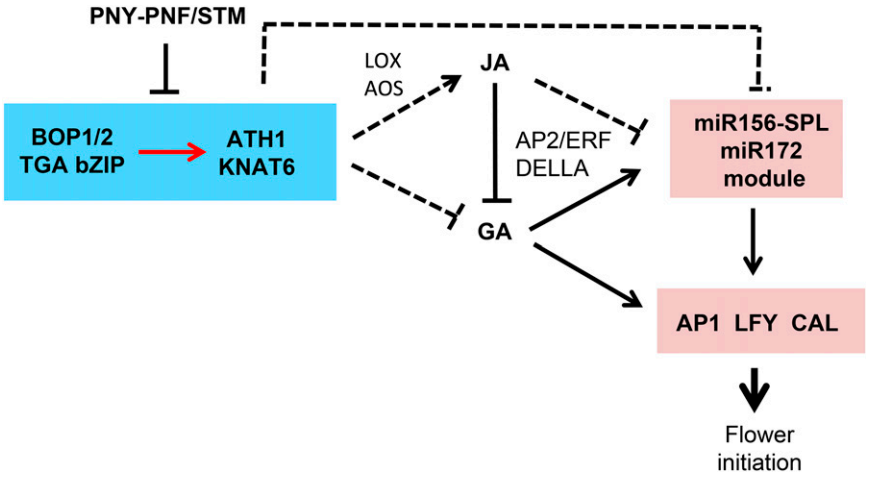

Figure 11. Summary and model. PNY-PNF/STM limits expression of *BOP1/2* and downstream effector *ATH1/KNAT6* to boundary domains flanking the IM. BOP1 acting through an unknown TGA bZIP cofactor directly activates *ATH1*, whereas promotion of *KNAT6* is indirect (red arrow). These products form a module that represses growth, meristem activity, and flowering by increasing JA content by transcriptional promotion of JA biosynthetic genes. Either directly or indirectly (dashed lines), we propose that misexpression of this pathway leads to down-regulation of GA pathway components and repression of the *miR156-SPL-miR172* module at one or more nodes in correlation with increased content of associated classes of floral repressors (e.g. DELLA, AP2-like, and AP2/ERF clades). Ultimately, *SPL* and *FD/FT* transcripts (not depicted) fail to accumulate, and activation of floral meristem identity genes *LFY*, *AP1*, and *CAL* required for flower initiation is blocked. Internode elongation is also blocked.

down-regulation of cellular carbohydrate metabolism, metabolic processes, and nitrogen metabolism, which potentially act to restrict Suc availability at the shoot apex (Supplemental Table S1). Parts of these changes were confirmed in *pny pnf* mutants, suggesting that resources are allocated toward defense in detriment to flowering.

Integration with GA Pathways

Our study also identifies GA pathway changes in *bop1-6D* and *pny pnf* mutants detrimental to flowering. In wild-type plants, bioactive GA content increases 100-fold at the transition (Eriksson et al., 2006), facilitating internode elongation and flowering by lowering the abundance of DELLA repressors (Mutasa-Göttgens and Hedden, 2009; Galvão et al., 2012; Porri et al., 2012; Yu et al., 2012). GA signals are partly integrated through the *miR156-SPL-miR172* module based on studies showing that GA/DELLA regulates *SPL3/4/6/9* transcription at the shoot apex independent of SOC1 (Galvão et al., 2012; Porri et al., 2012). Physical interaction of REPRESSOR OF GA1-3 DELLA with SPL9 interferes with activation of MADS-box flowering genes at the shoot apex and activation of *miR172b* in leaves, thereby maintaining AP2 and AP2-like repression of stem elongation and flowering (for review, see Wang, 2014). Other nodes of integration with the *miR156-SPL-miR172* module are likely given so that GA treatment does not markedly accelerate flowering in an *miR156* overexpression line (Yu et al., 2012). Transcriptional profiling in *bop1-6D* and *pny pnf* plants indicates complex changes affecting biosynthesis, catabolism, and/or signaling. Exogenous GA fails to restore flowering in *pny pnf* apices or internode elongation in *bop1-6D*, similar to transgenic plants overexpressing *ATH1* (Smith et al., 2004; Gómez-Mena and Sablowski, 2008; this study) and consistent with blockage at multiple steps. Four of five DELLA transcripts are significantly up-regulated in *pny pnf* apices, whereas *RGL3* is selectively up-regulated in *bop1-6D*. Transcript accumulation and steady-state level of protein show strong correlation in previous studies (Wild et al., 2012). Transgenic plants overexpressing DELLAs or DELLA proteins resistant to degradation are dwarf and late flowering, similar to *bop1-6D* plants (Dill et al., 2004; Hamama et al., 2012). RGL3, in particular, mediates cross talk between GA and JA pathways (Hou et al., 2013; Wild and Achard, 2013). JA selectively up-regulates RGL3, which binds to jasmonate ZIM-domain repressors of JA signaling to boost the immune response at the expense of growth (Wild et al., 2012; Wild and Achard, 2013).

JA Antagonism of Growth and Flowering

Our data raise the interesting possibility that JA antagonism of GA conditions *bop1-6D* and *pny pnf* phenotypic defects. GO analysis of differentially regulated genes in the *bop1-6D* transcriptome revealed significant enrichment of terms related to stress stimuli, including response to JA stimulus and to a lesser extent, responses to salicylic acid, ethylene, and abscisic acid stimuli, leading to the model that *BOP1* overexpression reprioritizes the plant for defense at the expense of growth. Higher levels of JA biosynthetic gene transcripts and

hormone are found in *bop1-6D* and *pny pnf* apices relative to wild-type control plants. These data support the findings by Canet et al. (2012), which identified BOP1/2 as essential for MeJA induced in priming for resistance to *Pseudomonas syringae* pv tomato DC3000. Plants exposed to high levels of jasmonate are stunted in growth of roots, leaves, and stems (Ellis et al., 2002; Cipollini, 2005; Bonaventure et al., 2007; Hyun et al., 2008; Zhang and Turner, 2008; Heinrich et al., 2013). Arabidopsis plants treated with jasmonate are also late flowering with short internodes and loss of apical dominance, giving an appearance similar to *bop1-6D* or *pny pnf*/+ mutants. Inhibitory effects of MeJA on flowering are also reported in *Pharbitis nil* (Maciejewska and Kopceiwicz, 2002; Maciejewska et al., 2004), *Chenopodium rubrum* (Albrechtová and Ullmann, 1994), and einkorn wheat (*Triticum monococcum*; Diallo et al., 2014). JA antagonism of growth or flowering has been linked to repression of GA biosynthesis (Magome et al., 2004; Heinrich et al., 2013), stabilization of DELLAs (Yang et al., 2012), and/or induction of AP2/ERF factors (Magome et al., 2008; Sun et al., 2008; Kang et al., 2011; Licausi et al., 2013). These data are consistent with JA contributing to *bop1-6D* and *pny pnf* developmental defects. Although inactivation of jasmonate biosynthesis by mutation of *AOS* fails to rescue flowering in *pny pnf* mutants, a small but significant increase in plant height and flowering time in *bop1-6D* supports this model.

Our data suggest that resources in *pny pnf* are reallocated toward defense at the expense of flowering and provide evidence for JA as a factor in modulating growth and meristem activity at boundaries.

MATERIALS AND METHODS

Plant Material and Growth Conditions

In the laboratory of S.R.H., Arabidopsis (*Arabidopsis thaliana*) plants were grown on soil or in vitro on minimal media (Haughn and Somerville, 1986) in growth chambers at 21°C under continuous light (24 h of light; intensity of 100 μmol m^{-2} s^{-1}), LD (16 h of light), or SD (8 h of light) conditions. In the laboratory of V.P., plants were grown in LD (16 h of light; 150 μmol m^{-2} s^{-1}) or SD (10 h of light; 1 h at 80 μmol m^{-2} s^{-1}, 8 h at 130 μmol m^{-2} s^{-1}, and 1 h at 80 μmol m^{-2} s^{-1}) conditions. The wild type was the Columbia (Col-0) ecotype of Arabidopsis. Mutant lines were obtained from the Arabidopsis Biological Resource Center (https://abrc.osu.edu/) or the Nottingham Arabidopsis Stock Centre (http://arabidopsis.info/). The *pny-40126* (SALK_40126), *pnf-96116* (SALK_96116), *bop1-3* (SALK_012994), *bop2-1* SALK_075879), *knat6-1* (SALK_047931), *knat6-2* (SALK_054482), *knat2-5* (SALK_099837), *ath1-1* (GABI-KAT_114A12), and *ath1-3* (SALK_113353) mutants have been described previously (Smith and Hake, 2003; Smith et al., 2004; Hepworth et al., 2005; Belles-Boix et al., 2006; Proveniers et al., 2007; Gómez-Mena and Sablowski, 2008). The *ath1-4* mutant was a gift from Lin Xu (Li et al., 2012). *35S:BOP2* and *bop1-6D* overexpression lines were described previously (Norberg et al., 2005). The *BOP1:GUS* and *BOP2:GUS* reporter lines were described previously (McKim et al., 2008; Xu et al., 2010). The *35S:KNAT6* overexpression line was also described previously (Shi et al., 2011).

Plant Genetics

Primers and strategies used for genotyping *bop1-3*, *bop2-1*, *knat6-2* (Khan et al., 2012b), *pny-40126* (Smith and Hake, 2003), *pnf-96116*, *pnf-33879* (Smith et al., 2004), *knat6-1*, *knat2-5* (Ragni et al., 2008), *ath1-1* (Proveniers et al., 2007), and *ath1-3* (Gómez-Mena and Sablowski, 2008) have been previously described. For genotyping *ath1-4*, primers ath1-4dCAPS-F and ath1-4dCAPS-R were used to amplify a 198-bp product from genomic DNA. Only the *ath1-4* product is cleaved by *Ssp*I to yield a 173-bp fragment. All mutant combinations were generated by crossing and confirmed by PCR genotyping. Primers are listed in Supplemental Table S2.

Phenotypic Analyses

For quantitative analysis of meristem arrest, seedlings were germinated on agar plates under SDs, transferred to soil on day 10, and scored for meristem arrest on day 25. Progenies from a selfed *pny pnf*/+ plant ($n = 624$) and a selfed *knat2 pny pnf*/+ plant ($n = 146$) were analyzed in parallel with wild-type plants and *bop1 bop2 pny pnf*, *ath1 pny pnf*, and *knat6 pny pnf* mutants ($n = 144$). Quantitative analyses of inflorescence phenotypes were performed with 8-week-old plants grown under LDs. Average height, internode length, and rosette paraclade number were determined for 10 plants per genotype as previously described (Ragni et al., 2008). Flowering time was scored for at least 24 plants per genotype by monitoring the date of apex emergence, because *bop1 bop2* mutants initiate leaves at a reduced rate (Norberg et al., 2005). Seeds were germinated directly on soil under LDs. All phenotypic analyses were performed at least twice under independent growth conditions with similar results.

In Situ Hybridization and Localization of GUS Activity

Plants for analysis were grown under SDs for 3 weeks followed by 15 d in continuous light before harvesting tissue. We used in situ hybridization to monitor gene expression, because control sequences for expression of *KNAT2:GUS* and *KNAT6:GUS* reporters in IMs are missing (Khan et al., 2012b). Tissue fixation, embedding, and sectioning were carried out as described (Nikovics et al., 2006) with minor changes. Hybridization was performed overnight using the following buffer: 50% (v/v) formamide, 10% (w/v) dextran sulfate, 1× Denhardts, 0.3 M NaCl, 10 mM Tris HCl, pH 8, 1 mM EDTA, and 5 mg mL^{-1} transfer RNA. Primers used to make *KNAT6*, *KNAT2*, *BOP2*, and *ATH1* antisense probes are as listed in Supplemental Table S2.

Tissues were analyzed for *BOP1:GUS* activity as described (Sieburth and Meyerowitz, 1997) with minor changes. Stained tissues were embedded in Paraplast Plus (Sigma) processed using *tert*-butanol instead of xylenes. Sections (10 μm) were cut from embedded tissue, affixed to glass slides, and dewaxed with *tert*-butanol before imaging.

Construction of D35S:BOP1-GR, BOP1p-BOP1-GR, D35S:ATH1, and ATH1p:GUS Transgenic Lines

A translational fusion of BOP1 to the steroid-binding domain of the rat glucocorticoid receptor was generated. Treatment with DEX leads to translocation of the GR fusion protein from the cytoplasm to the nucleus as a way of controlling transcription factor activity (Lloyd et al., 1994). The *BOP1* coding sequence lacking a stop codon was fused in frame to the GR fragment using overlap extension mutagenesis (Heckman and Pease, 2007). The resulting product was cloned into pCR-BluntII-TOPO (Invitrogen) to create B359. For all cloning steps involving amplification by PCR, iProof was used as the polymerase (BioRad), and cloned inserts were sequenced to ensure fidelity.

To create *D35S:BOP1-GR*, the *BOP1-GR* fusion gene present in B359 was amplified by PCR using CDS-BOP1-F and GR-R as the primers. The resulting product was modified to contain dATP overhangs and transferred to the Gateway-compatible entry vector pCR8/GW/TOPO (Invitrogen). LR clonase (Invitrogen) was used to move the insert to a pSM-3-based destination vector containing a double 35S Cauliflower mosaic virus (CaMV) promoter (*D35S*) and Nos terminator (pBAR, gift of C. Douglas). Wild-type plants were transformed by floral dipping (Clough and Bent, 1998) using the *Agrobacterium* spp. strain C58C1 pGV3101 pMP90 (Koncz and Schell, 1986). Hygromycin-resistant primary transformants were selected on agar plates containing 10 μm of DEX. After transfer to soil, plants were sprayed daily with 10 μm of DEX to induce nuclear localization of the BOP1-GR fusion protein. Homozygous progeny from one DEX-induced *D35S:BOP1-GR* line with a dwarf phenotype (line 9) was used for all subsequent experiments.

The *D35S:BOP1-GR* transgene failed to complement *bop1 bop2* plants, presumably because the *35S CaMV* promoter fails to provide the correct range of tissue expression. To confirm activity of the fusion protein and for use in ChIP experiments, the *BOP1-GR* fusion gene was expressed under control of the *BOP1* native promoter in *bop1 bop2* plants. The transgene was created in two steps. The *BOP1* promoter present in *pBOP1:GUS* (McKim et al., 2008) was

amplified by PCR using primers 4H-4kb-*Eco*R1-F1 and 4H-4kb-*Xma*I-R1 that incorporated restriction sites at their 5′ ends. The resulting product was digested with *Eco*R1 and *Xma*I and cloned into the corresponding sites of the binary vector pBAR (gift from laboratory of J. Dangl) to create B149. The *BOP1-GR* fusion gene present in B359 was amplified by PCR using primers *Xma*I-BOP1-F and BOP1-*Xma*I-R. The resulting product was digested with *Xma*I and cloned into the corresponding site of B149 to create pBAR/BOP1prom:BOP1-GR. The transgene was introduced into *bop1 bop2* plants by floral dipping. Primary transformants resistant to glufosinate-ammonium were selected on soil using the herbicide FINALE (Farnam Companies). Three independent lines were used to assess complementation of *bop1 bop2* mutant phenotypes. T2 seeds were sown on agar plates containing phosphinothricin with or without 5 μm of DEX. Plants were transferred to soil and sprayed daily with mock or DEX solution until maturity. Complementation of leaf, floral patterning, and floral organ abscission was observed in all DEX-treated lines (Supplemental Fig. S7).

To make the *D35S:ATH1* transgene, the *ATH1* coding sequence was amplified by PCR from cloned complementary DNA (cDNA) template using ATH1-CDS-F1 and ATH1-CDS-F1 as the primers. The resulting fragment was cloned into the entry vector pCR8/GW/TOPO and transferred into the pSM-3-based destination vector as described above. Wild-type plants were transformed by floral dipping. Transformants were selected on agar plates containing hygromycin. Phenotypes were scored in the T1 generation.

To create *ATH1* promoter fusions to a GUS reporter gene, fragments containing 3.3 or 2 kb of sequence upstream of the *ATH1* translation start site were amplified by PCR from genomic DNA template (BAC MSD21) and fused to the coding region of the beta-glucuronidase (uidA or GUS) gene. Primers incorporating *Bam*HI and *Nco*I restriction sites at their 5′ ends facilitated directional cloning. Products were cloned into pCR-BluntII-TOPO for propagation. Inserts were released by digestion with *Bam*HI and *Nco*I and ligated into the corresponding sites of pGCO:GUS (Hepworth et al., 2002). *Agrobacterium* spp. was cotransformed with pSOUP (Hellens et al., 2000). Wild-type plants were transformed by floral dipping, and glufosinate-ammonium-resistant primary transformants were selected on soil. Cloning primers are listed in Supplemental Table S2.

ChIP Experiments

ChIP was performed as described (Chakravarthy et al., 2003) using an anti-GR antibody (catalog no. 1002; Santa Cruz Biotechnology) and mock- or DEX-treated *BOP1p:BOP1-GR bop1 bop2* plants grown under LDs. Seeds were germinated on agar plates containing phosphinothricin with or without 10 μm of DEX. After transfer to soil, plants were sprayed daily with mock (0.04% ethanol) or DEX solutions. Leaf tissue was collected from 4-week-old flowering plants for analysis. Quantification of immunoprecipitated DNA by qRT-PCR was performed as previously described (Boyle et al., 2009). Primers were as listed in Supplemental Table S3.

Microarray Experimental Design, Hybridization, and Analysis

Tissue for profiling was harvested from the first expanded internodes of wild-type and *bop1-6D* flowering plants grown under continuous light. RNA was extracted from four biological replicates per genotype using an RNeasy Plant Mini Kit (Qiagen). The mRNA was amplified according to the protocol described in the MessageAmp aRNA Kit (catalog no. 1750; Ambion). To produce incorporated antisense mRNA, aminoallyl-UTP was incorporated into the newly synthesized RNA; 3 μL of aminoallyl-UTP (50 mM) plus 2 μL of UTP (75 mM) instead of 4 μL of UTP were added during the aRNA amplification. Labeling, hybridization, and scanning were performed as described (Xiang et al., 2011). To normalize for bias in dye labeling, two biological replicates were labeled with [5′-^{32}P] cytosine-3′-P (Cy3), and two were labeled with Cy5. Experiments were carried out using Arabidopsis 70-mer oligo microarray slides (http://ag.arizona.edu/microarray). Two-color microarray data were preprocessed with the marray package (version 1.42.0) implemented in R/BioConductor (R Development Core Team; Gentleman et al., 2004; https://www.bioconductor.org) using the background correction method normexp (offset = 50) and normalize within arrays method loess. Differentially expressed genes were identified by *P* values, fold changes, and contrasts using linear models for microarrays (Smyth, 2005) and included a dye effect assessment implemented in R/BioConductor.

qRT-PCR

Total RNA was isolated using Trizol Reagent (Invitrogen) from dissected apices of the wild type and mutants. Plants grown under SDs were harvested on day 25 (SD) or transferred to LDs to induce flowering and harvested after 12 d (LD). Dissected apices were <0.5 cm tall, with the majority of surrounding leaves >0.2 cm removed. Tissues were collected in the subjective afternoon for all samples (after 9–12 h of light in a 16-h cycle). cDNA was generated using 1 μg of RNA as the template under following conditions: step 1: 70°C for 5 min; step 2: 50°C for 60 min; and step 3: 70°C for 15 min. qRT-PCR was carried out as described (Khan et al., 2012b) with the following changes. Reactions in triplicate containing 2 μL of 10-fold diluted cDNA, except for *LFY* and *AP1* reactions, which required 4 μL of diluted cDNA, gene-specific primers (Supplemental Table S3), and POWER SYBR Green PCR Mastermix (Invitrogen) were carried out using a StepOnePlus Thermocycler (Applied Biosystems). *GLYCERALDE-3-PHOSPHATE DEHYDROGENASE C* was used as a normalization control. Quantification of *miR156* mRNA was performed as described (Porri et al., 2012). Data shown are the average of three biological replicates conducted using separate growth trials and independently isolated RNA samples. Error bars indicate SEM.

For DEX induction experiments, total RNA was prepared from internodes of 4-week-old flowering plants expressing the *D35S:BOP1-GR* transgene. Internodes were harvested from primary and secondary inflorescences of five to six plants starting at the bottom above the first silique and going all of the way up to where internodes were too small to collect. Tissue was excised with a new razor blade on parafilm, frozen in liquid nitrogen, and stored at −80°C until further analysis. Plants were treated continuously with mock (0.12% ethanol), 30 μm of DEX, 50 μm of CHX, or 30 μm of DEX and 50 μm of CHX for 2, 4, or 24 h by inverting inflorescences into containers of solution. For long-term treatments, seedlings were germinated on agar plates containing 10 μm of DEX. After transplanting to soil, plants were sprayed daily with a solution of mock (0.04% ethanol) or DEX for 4 weeks until tissue was harvested for RNA extraction. Values were normalized to *EUKARYOTIC TRANSLATION INITIATION FACTOR 4A1* transcript (At3g13920), the mock control for DEX treatments, and the CHX control for DEX and CHX treatments to correct for negative effects of CHX on the transcription of *BOP1* target genes (Jun et al., 2010; Nakamichi et al., 2010). Data shown are the average of three biological replicates conducted using independently isolated RNA samples. Error bars indicate SEM.

Hormone Treatments

To analyze the effect of GA on growth, 10-d-old seedlings grown under continuous light were sprayed daily with GA (100 μm of GA_3 and 0.02% Silwett L-77) or a mock (0.02% Silwett L-77) solution until maturity (Hay et al., 2002). To examine the effect of JA on growth, 7-d-old seedlings grown under LDs were sprayed daily with MeJA (100 μm of MeJA and 0.02% Silwett L-77) or a mock (0.02% Silwett L-77) solution until maturity (Canet et al., 2012). MeJA-treated plants were covered with a plastic dome for 1 h after treatments, and solutions were made fresh once a week. Flowering time was determined by scoring the date of apex emergence. At least 24 plants per genotype were monitored.

JA Measurements

For measurement of JA, wild-type, *bop1 bop2*, and *bop1-6D* plants were grown for 6 to 7 weeks under LDs. Pools of 30 apices (buds and internodes) were used for each replicate (100 mg of fresh material). Wild-type and *pny pnf* plants were grown for 4 weeks under SDs. Pools of 30 apices (90 mg of fresh material) were used for each replicate. Three biological replicates were collected for each condition. Tissues were directly harvested in liquid nitrogen. Tissues were ground in liquid nitrogen and lyophilized. For each sample, 10 mg of freeze-dried powder was extracted with 0.8 mL of acetone:water:acetic acid (80:19:1, v/v/v) containing 2 ng of [5-2H] JA (CDN Isotopes CIL Cluzeau; Le Roux et al., 2014). The extract was vigorously shaken for 1 min, sonicated for 1 min at 25 Hz, shaken for 10 min at 4°C in a Thermomixer (Eppendorf), and then centrifuged (8,000*g* at 4°C for 10 min). The supernatants were collected, and the pellets were reextracted twice with 0.4 mL of the same extraction solution; then, they were vigorously shaken (1 min) and sonicated (1 min; 25 Hz). After the centrifugations, the three supernatants were pooled and dried (final volume of 1.6 mL). Each dry extract was dissolved in 140 μL of acetonitrile:water (50:50, v/v), filtered, and analyzed using a Waters Acquity Ultra Performance Liquid Chromatograph coupled to a Waters Xevo Triple Quadrupole Mass Spectrometer TQS. The compounds were separated on a reverse-phase column (100 mm × 2.1 mm × 3 μm particle size; Uptisphere C18 UP3HDO; Interchim) using a flow rate of 0.4 mL min^{-1} and a binary gradient: 0.1% (v/v) acetic acid in water and acetonitrile with 0.1% acetic acid. For JA, the following binary gradient (0.1% [v/v] acetic acid in water) was used: 0 min, 98%; 3 min, 70%;

7.5 min, 50%; 8.5 min, 5%; 9.6 min, 0%; 13.2 min, 98%; and 15.7 min, 98%. Mass spectrometry was conducted in electrospray and multiple reaction monitoring scanning mode in negative ion mode. Relevant instrumental parameters were set as follows: capillary, 1.5 kV (negative mode); source block and desolvation gas temperatures, 130°C and 500°C, respectively. Nitrogen was used to assist the cone and desolvation (150 and 800 L h^{-1}, respectively). Argon was used as the collision gas at a flow of 0.18 mL min^{-1}. The parameters used for multiple reaction monitoring quantification of JA are described in Le Roux et al., 2014. Samples were reconstituted in 140 μL of 50:50 (v/v) acetonitrile:water per 1 mL of injected volume. The JA limit of detection and limit of quantification were extrapolated from calibration curves and samples using the Quantify module of MassLynx software (version 4.1). The amount of JA was expressed as a ratio of peak areas (209 > 62/214 > 62) per dry weight because of impurities contained in the D5 JA standard.

Sequence data from this article can be found in the EMBL/GenBank data libraries under accession numbers At1g70510 (*KNAT2*), At1g23380 (*KNAT6*), At5g02030 (*PNY*), At2g27990 (*PNF*), At3g57130 (*BOP1*), At2g41370 (*BOP2*), and At4g32980 (*ATH1*).

Supplemental Data

The following supplemental materials are available.

Supplemental Figure S1. Ectopic expression of *KNAT6* and *ATH1* mimics *pny* and *pny pnf*/+ phenotype.

Supplemental Figure S2. *ATH1* map and characterization of mutant alleles.

Supplemental Figure S3. Phenotypes of other mutant combinations.

Supplemental Figure S4. Quantitative phenotypic analyses of *bop1 bop2 pny pnf*, *ath1 pny pnf*, and *knat6 pny pnf* mutants.

Supplemental Figure S5. *BOP1:GUS* expression in Col-0 and *pny pnf* apices.

Supplemental Figure S6. *BOP2*, *ATH1*, *KNAT2*, and *KNAT6* expression in *pny* and *pnf* apices.

Supplemental Figure S7. Complementation of *bop1 bop2* mutant by *BOP1p::BOP1-GR* construct.

Supplemental Table S1. GO classification of differentially expressed genes in *bop1-6D* versus Col-0 internode microarrays.

Supplemental Table S2. List of general primers.

Supplemental Table S3. List of primers for qRT-PCR.

ACKNOWLEDGMENTS

We thank the Salk Institute Genomic Analysis Laboratory for providing the sequence-indexed Arabidopsis T-DNA insertion mutants, Hervé Ferry and Bruno Letarnec for greenhouse management, Gregory Mouille and the Institut Jean-Pierre Bourgin Green Chemistry Platform for the quantification of JA, Alex Edwards for *BOP1p::BOP1-GR bop1 bop2* complementation data, and Jin Cheong and Mike Bush for constructing the *bop1 bop2 pny pnf* quadruple mutant. This article is dedicated to the memory of J.-P.R.

Received June 22, 2015; accepted September 25, 2015; published September 28, 2015.

LITERATURE CITED

Abe M, Kobayashi Y, Yamamoto S, Daimon Y, Yamaguchi A, Ikeda Y, Ichinoki H, Notaguchi M, Goto K, Araki T (2005) FD, a bZIP protein mediating signals from the floral pathway integrator FT at the shoot apex. Science **309:** 1052–1056

Aichinger E, Kornet N, Friedrich T, Laux T (2012) Plant stem cell niches. Annu Rev Plant Biol **63:** 615–636

Aida M, Tasaka M (2006) Genetic control of shoot organ boundaries. Curr Opin Plant Biol **9:** 72–77

Albrechtová JTP, Ullmann J (1994) Methyl jasmonate inhibits growth and flowering in *Chenopodium rubrum*. Biol Plant **36:** 317–319

Amasino RM, Michaels SD (2010) The timing of flowering. Plant Physiol **154:** 516–520

Andrés F, Coupland G (2012) The genetic basis of flowering responses to seasonal cues. Nat Rev Genet **13:** 627–639

Andrés F, Romera-Branchat M, Martínez-Gallegos R, Patel V, Schneeberger K, Jang S, Altmüller J, Nürnberg P, Coupland G (2015) Floral induction in Arabidopsis by FLOWERING LOCUS T requires direct repression of *BLADE-ON-PETIOLE* genes by the homeodomain protein PENNYWISE. Plant Physiol **169:** 2187–2199

Aukerman MJ, Sakai H (2003) Regulation of flowering time and floral organ identity by a MicroRNA and its *APETALA2*-like target genes. Plant Cell **15:** 2730–2741

Belles-Boix E, Hamant O, Witiak SM, Morin H, Traas J, Pautot V (2006) *KNAT6*: an *Arabidopsis* homeobox gene involved in meristem activity and organ separation. Plant Cell **18:** 1900–1907

Bernier G (1988) The control of floral evocation and morphogenesis. Ann Rev Plant Physiol Plant Mol Biol **39:** 175–219

Bonaventure G, Gfeller A, Proebsting WM, Hörtensteiner S, Chételat A, Martinoia E, Farmer EE (2007) A gain-of-function allele of TPC1 activates oxylipin biogenesis after leaf wounding in Arabidopsis. Plant J **49:** 889–898

Bowman J, Alvarez J, Weigel D, Meyerowitz E (1993) Control of flower development in *Arabidopsis thaliana* by *APETALA1* and interacting genes. Development **119:** 721–743

Boyle P, Le Su E, Rochon A, Shearer HL, Murmu J, Chu JY, Fobert PR, Després C (2009) The BTB/POZ domain of the *Arabidopsis* disease resistance protein NPR1 interacts with the repression domain of TGA2 to negate its function. Plant Cell **21:** 3700–3713

Byrne ME, Barley R, Curtis M, Arroyo JM, Dunham M, Hudson A, Martienssen RA (2000) *Asymmetric leaves1* mediates leaf patterning and stem cell function in Arabidopsis. Nature **408:** 967–971

Byrne ME, Groover AT, Fontana JR, Martienssen RA (2003) Phyllotactic pattern and stem cell fate are determined by the Arabidopsis homeobox gene *BELLRINGER*. Development **130:** 3941–3950

Canet JV, Dobón A, Fajmonová J, Tornero P (2012) The *BLADE-ON-PETIOLE* genes of Arabidopsis are essential for resistance induced by methyl jasmonate. BMC Plant Biol **12:** 199

Chakravarthy S, Tuori RP, D'Ascenzo MD, Fobert PR, Després C, Martin GB (2003) The tomato transcription factor Pti4 regulates defense-related gene expression via GCC box and non-GCC box *cis* elements. Plant Cell **15:** 3033–3050

Cho SH, Coruh C, Axtell MJ (2012) miR156 and miR390 regulate tasiRNA accumulation and developmental timing in *Physcomitrella patens*. Plant Cell **24:** 4837–4849

Cipollini D (2005) Interactive effects of lateral shading and jasmonic acid on morphology, phenology, seed production,and defense traits in *Arabidopsis thaliana*. Int J Plant Sci **166:** 955–959

Clark SE, Jacobsen SE, Levin JZ, Meyerowitz EM (1996) The *CLAVATA* and *SHOOT MERISTEMLESS* loci competitively regulate meristem activity in Arabidopsis. Development **122:** 1567–1575

Clough SJ, Bent AF (1998) Floral dip: a simplified method for *Agrobacterium*-mediated transformation of *Arabidopsis thaliana*. Plant J **16:** 735–743

Corbesier L, Vincent C, Jang S, Fornara F, Fan Q, Searle I, Giakountis A, Farrona S, Gissot L, Turnbull C, et al (2007) FT protein movement contributes to long-distance signaling in floral induction of Arabidopsis. Science **316:** 1030–1033

Cui LG, Shan JX, Shi M, Gao JP, Lin HX (2014) The *miR156-SPL9-DFR* pathway coordinates the relationship between development and abiotic stress tolerance in plants. Plant J **80:** 1108–1117

Després C, DeLong C, Glaze S, Liu E, Fobert PR (2000) The *Arabidopsis* NPR1/NIM1 protein enhances the DNA binding activity of a subgroup of the TGA family of bZIP transcription factors. Plant Cell **12:** 279–290

Diallo AO, Agharbaoui Z, Badawi MA, Ali-Benali MA, Moheb A, Houde M, Sarhan F (2014) Transcriptome analysis of an *mvp* mutant reveals important changes in global gene expression and a role for methyl jasmonate in vernalization and flowering in wheat. J Exp Bot **65:** 2271–2286

Dill A, Thomas SG, Hu J, Steber CM, Sun TP (2004) The *Arabidopsis* F-box protein SLEEPY1 targets gibberellin signaling repressors for gibberellin-induced degradation. Plant Cell **16:** 1392–1405

Ellis C, Karafyllidis I, Wasternack C, Turner JG (2002) The *Arabidopsis* mutant *cev1* links cell wall signaling to jasmonate and ethylene responses. Plant Cell **14:** 1557–1566

Endrizzi K, Moussian B, Haecker A, Levin JZ, Laux T (1996) The *SHOOT MERISTEMLESS* gene is required for maintenance of undifferentiated cells in Arabidopsis shoot and floral meristems and acts at a different regulatory level than the meristem genes *WUSCHEL* and *ZWILLE*. Plant J **10:** 967–979

Eriksson S, Böhlenius H, Moritz T, Nilsson O (2006) GA_4 is the active gibberellin in the regulation of *LEAFY* transcription and *Arabidopsis* floral initiation. Plant Cell **18:** 2172–2181

Etchells JP, Moore L, Jiang WZ, Prescott H, Capper R, Saunders NJ, Bhatt AM, Dickinson HG (2012) A role for *BELLRINGER* in cell wall development is supported by loss-of-function phenotypes. BMC Plant Biol **12:** 212

Fode B, Siemsen T, Thurow C, Weigel R, Gatz C (2008) The *Arabidopsis* GRAS protein SCL14 interacts with class II TGA transcription factors and is essential for the activation of stress-inducible promoters. Plant Cell **20:** 3122–3135

Galvão VC, Horrer D, Küttner F, Schmid M (2012) Spatial control of flowering by DELLA proteins in *Arabidopsis thaliana*. Development **139:** 4072–4082

Gentleman RC, Carey VJ, Bates DM, Bolstad B, Dettling M, Dudoit S, Ellis B, Gautier L, Ge Y, Gentry J, et al (2004) Bioconductor: open software development for computational biology and bioinformatics. Genome Biol **5:** R80

Gómez-Mena C, Sablowski R (2008) *ARABIDOPSIS THALIANA HOMEOBOX GENE1* establishes the basal boundaries of shoot organs and controls stem growth. Plant Cell **20:** 2059–2072

Ha CM, Jun JH, Nam HG, Fletcher JC (2007) *BLADE-ON-PETIOLE1* and *2* control *Arabidopsis* lateral organ fate through regulation of LOB domain and adaxial-abaxial polarity genes. Plant Cell **19:** 1809–1825

Hamama L, Naouar A, Gala R, Voisine L, Pierre S, Jeauffre J, Cesbron D, Leplat F, Foucher F, Dorion N, et al (2012) Overexpression of RoDELLA impacts the height, branching, and flowering behaviour of Pelargonium × domesticum transgenic plants. Plant Cell Rep **31:** 2015–2029

Hamant O, Pautot V (2010) Plant development: a TALE story. C R Biol **333:** 371–381

Haughn GW, Somerville C (1986) Sulfonylurea-resistant mutants of *Arabidopsis thaliana*. Mol Gen Genet **204:** 430–434

Hay A, Kaur H, Phillips A, Hedden P, Hake S, Tsiantis M (2002) The gibberellin pathway mediates KNOTTED1-type homeobox function in plants with different body plans. Curr Biol **12:** 1557–1565

Hay A, Tsiantis M (2010) KNOX genes: versatile regulators of plant development and diversity. Development **137:** 3153–3165

Heckman KL, Pease LR (2007) Gene splicing and mutagenesis by PCR-driven overlap extension. Nat Protoc **2:** 924–932

Heinrich M, Hettenhausen C, Lange T, Wünsche H, Fang J, Baldwin IT, Wu J (2013) High levels of jasmonic acid antagonize the biosynthesis of gibberellins and inhibit the growth of *Nicotiana attenuata* stems. Plant J **73:** 591–606

Hellens RP, Edwards EA, Leyland NR, Bean S, Mullineaux PM (2000) pGreen: a versatile and flexible binary Ti vector for *Agrobacterium*-mediated plant transformation. Plant Mol Biol **42:** 819–832

Hepworth SR, Valverde F, Ravenscroft D, Mouradov A, Coupland G (2002) Antagonistic regulation of flowering-time gene *SOC1* by CONSTANS and FLC via separate promoter motifs. EMBO J **21:** 4327–4337

Hepworth SR, Zhang Y, McKim S, Li X, Haughn GW (2005) BLADE-ON-PETIOLE–dependent signaling controls leaf and floral patterning in *Arabidopsis*. Plant Cell **17:** 1434–1448

Hou X, Ding L, Yu H (2013) Crosstalk between GA and JA signaling mediates plant growth and defense. Plant Cell Rep **32:** 1067–1074

Hu J, Mitchum MG, Barnaby N, Ayele BT, Ogawa M, Nam E, Lai WC, Hanada A, Alonso JM, Ecker JR, et al (2008) Potential sites of bioactive gibberellin production during reproductive growth in *Arabidopsis*. Plant Cell **20:** 320–336

Huijser P, Schmid M (2011) The control of developmental phase transitions in plants. Development **138:** 4117–4129

Hyun Y, Choi S, Hwang HJ, Yu J, Nam SJ, Ko J, Park JY, Seo YS, Kim EY, Ryu SB, et al (2008) Cooperation and functional diversification of two closely related galactolipase genes for jasmonate biosynthesis. Dev Cell **14:** 183–192

Izawa T, Foster R, Chua NH (1993) Plant bZIP protein DNA binding specificity. J Mol Biol **230:** 1131–1144

Jaeger KE, Wigge PA (2007) FT protein acts as a long-range signal in Arabidopsis. Curr Biol **17:** 1050–1054

Jun JH, Ha CM, Fletcher JC (2010) BLADE-ON-PETIOLE1 coordinates organ determinacy and axial polarity in *Arabidopsis* by directly activating ASYMMETRIC LEAVES2. Plant Cell **22:** 62–76

Jung JH, Ju Y, Seo PJ, Lee JH, Park CM (2012) The SOC1-SPL module integrates photoperiod and gibberellic acid signals to control flowering time in Arabidopsis. Plant J **69:** 577–588

Jung JH, Seo YH, Seo PJ, Reyes JL, Yun J, Chua NH, Park CM (2007) The GIGANTEA-regulated microRNA172 mediates photoperiodic flowering independent of CONSTANS in *Arabidopsis*. Plant Cell **19:** 2736–2748

Kang HG, Kim J, Kim B, Jeong H, Choi SH, Kim EK, Lee HY, Lim PO (2011) Overexpression of *FTL1/DDF1*, an AP2 transcription factor, enhances tolerance to cold, drought, and heat stresses in *Arabidopsis thaliana*. Plant Sci **180:** 634–641

Kanrar S, Bhattacharya M, Arthur B, Courtier J, Smith HMS (2008) Regulatory networks that function to specify flower meristems require the function of homeobox genes PENNYWISE and POUND-FOOLISH in Arabidopsis. Plant J **54:** 924–937

Kanrar S, Onguka O, Smith HMS (2006) Arabidopsis inflorescence architecture requires the activities of KNOX-BELL homeodomain heterodimers. Planta **224:** 1163–1173

Khan M, Tabb P, Hepworth SR (2012a) *BLADE-ON-PETIOLE1* and *2* regulate Arabidopsis inflorescence architecture in conjunction with homeobox genes *KNAT6* and *ATH1*. Plant Signal Behav **7:** 788–792

Khan M, Xu H, Hepworth SR (2014) *BLADE-ON-PETIOLE* genes: setting boundaries in development and defense. Plant Sci **215-216:** 157–171

Khan M, Xu M, Murmu J, Tabb P, Liu Y, Storey K, McKim SM, Douglas CJ, Hepworth SR (2012b) Antagonistic interaction of BLADE-ON-PETIOLE1 and 2 with BREVIPEDICELLUS and PENNYWISE regulates Arabidopsis inflorescence architecture. Plant Physiol **158:** 946–960

Kim JJ, Lee JH, Kim W, Jung HS, Huijser P, Ahn JH (2012) The *microRNA156-SQUAMOSA PROMOTER BINDING PROTEIN-LIKE3* module regulates ambient temperature-responsive flowering via *FLOWERING LOCUS T* in Arabidopsis. Plant Physiol **159:** 461–478

Koncz C, Schell J (1986) The promoter of TL-DNA gene *5* controls the tissue-specific expression of chimeric genes carried by a novel type of *Agrobacterium* binary vector. Mol Gen Genet **204:** 383–396

Lal S, Pacis LB, Smith HM (2011) Regulation of the *SQUAMOSA PROMOTER-BINDING PROTEIN-LIKE genes/microRNA156* module by the homeodomain proteins PENNYWISE and POUND-FOOLISH in Arabidopsis. Mol Plant **4:** 1123–1132

Le Roux C, Del Prete S, Boutet-Mercey S, Perreau F, Balagué C, Roby D, Fagard M, Gaudin V (2014) The hnRNP-Q protein LIF2 participates in the plant immune response. PLoS One **9:** e99343

Li Y, Pi L, Huang H, Xu L (2012) ATH1 and KNAT2 proteins act together in regulation of plant inflorescence architecture. J Exp Bot **63:** 1423–1433

Licausi F, Ohme-Takagi M, Perata P (2013) APETALA2/Ethylene Responsive Factor (AP2/ERF) transcription factors: mediators of stress responses and developmental programs. New Phytol **199:** 639–649

Lincoln C, Long J, Yamaguchi J, Serikawa K, Hake S (1994) A *knotted1*-like homeobox gene in *Arabidopsis* is expressed in the vegetative meristem and dramatically alters leaf morphology when overexpressed in transgenic plants. Plant Cell **6:** 1859–1876

Lloyd AM, Schena M, Walbot V, Davis RW (1994) Epidermal cell fate determination in Arabidopsis: patterns defined by a steroid-inducible regulator. Science **266:** 436–439

Long JA, Moan EI, Medford JI, Barton MK (1996) A member of the KNOTTED class of homeodomain proteins encoded by the *STM* gene of Arabidopsis. Nature **379:** 66–69

Maciejewska B, Kopceiwicz J (2002) Inhibitory effect of methyl jasmonate on flowering and elongation growth in *Pharbitis nil*. J Plant Growth Regul **21:** 216–223

Maciejewska BD, Kesy J, Zielinska M, Kopcewicz J (2004) Jasmonates inhibit flowering in short-day plant *Pharbitis nil*. Plant Growth Regul **43:** 1–8

Magome H, Yamaguchi S, Hanada A, Kamiya Y, Oda K (2004) *dwarf and delayed-flowering 1*, a novel Arabidopsis mutant deficient in gibberellin biosynthesis because of overexpression of a putative AP2 transcription factor. Plant J **37:** 720–729

Magome H, Yamaguchi S, Hanada A, Kamiya Y, Oda K (2008) The DDF1 transcriptional activator upregulates expression of a gibberellin-deactivating gene, *GA2ox7*, under high-salinity stress in Arabidopsis. Plant J **56:** 613–626

Mathieu J, Warthmann N, Küttner F, Schmid M (2007) Export of FT protein from phloem companion cells is sufficient for floral induction in Arabidopsis. Curr Biol **17:** 1055–1060

Mathieu J, Yant LJ, Mürdter F, Küttner F, Schmid M (2009) Repression of flowering by the miR172 target SMZ. PLoS Biol **7:** e1000148

Matsoukas IG, Massiah AJ, Thomas B (2012) Florigenic and antflorigenic signaling in plants. Plant Cell Physiol **53:** 1827–1842

McKim SM, Stenvik GE, Butenko MA, Kristiansen W, Cho SK, Hepworth SR, Aalen RB, Haughn GW (2008) The *BLADE-ON-PETIOLE* genes are essential for abscission zone formation in Arabidopsis. Development **135:** 1537–1546

Mele G, Ori N, Sato Y, Hake S (2003) The *knotted1*-like homeobox gene BREVIPEDICELLUS regulates cell differentiation by modulating metabolic pathways. Genes Dev **17:** 2088–2093

Mutasa-Göttgens E, Hedden P (2009) Gibberellin as a factor in floral regulatory networks. J Exp Bot **60:** 1979–1989

Nakamichi N, Kiba T, Henriques R, Mizuno T, Chua NH, Sakakibara H (2010) PSEUDO-RESPONSE REGULATORS 9, 7, and 5 are transcriptional repressors in the *Arabidopsis* circadian clock. Plant Cell **22:** 594–605

Navarro L, Bari R, Achard P, Lisón P, Nemri A, Harberd NP, Jones JDG (2008) DELLAs control plant immune responses by modulating the balance of jasmonic acid and salicylic acid signaling. Curr Biol **18:** 650–655

Nikovics K, Blein T, Peaucelle A, Ishida T, Morin H, Aida M, Laufs P (2006) The balance between the *MIR164A* and *CUC2* genes controls leaf margin serration in *Arabidopsis*. Plant Cell **18:** 2929–2945

Norberg M, Holmlund M, Nilsson O (2005) The *BLADE ON PETIOLE* genes act redundantly to control the growth and development of lateral organs. Development **132:** 2203–2213

Park JH, Halitschke R, Kim HB, Baldwin IT, Feldmann KA, Feyereisen R (2002) A knock-out mutation in allene oxide synthase results in male sterility and defective wound signal transduction in Arabidopsis due to a block in jasmonic acid biosynthesis. Plant J **31:** 1–12

Peaucelle A, Louvet R, Johansen JN, Salsac F, Morin H, Fournet F, Belcram K, Gillet F, Höfte H, Laufs P, et al (2011) The transcription factor BELLRINGER modulates phyllotaxis by regulating the expression of a pectin methylesterase in Arabidopsis. Development **138:** 4733–4741

Porri A, Torti S, Romera-Branchat M, Coupland G (2012) Spatially distinct regulatory roles for gibberellins in the promotion of flowering of Arabidopsis under long photoperiods. Development **139:** 2198–2209

Proveniers M (2013) Sugars speed up the circle of life. eLife **2:** e00625

Proveniers M, Rutjens B, Brand M, Smeekens S (2007) The Arabidopsis TALE homeobox gene *ATH1* controls floral competency through positive regulation of *FLC*. Plant J **52:** 899–913

Ragni L, Belles-Boix E, Günl M, Pautot V (2008) Interaction of *KNAT6* and *KNAT2* with *BREVIPEDICELLUS* and *PENNYWISE* in *Arabidopsis* inflorescences. Plant Cell **20:** 888–900

Rutjens B, Bao D, van Eck-Stouten E, Brand M, Smeekens S, Proveniers M (2009) Shoot apical meristem function in Arabidopsis requires the combined activities of three BEL1-like homeodomain proteins. Plant J **58:** 641–654

Schindler U, Beckmann H, Cashmore AR (1992) TGA1 and G-box binding factors: two distinct classes of *Arabidopsis* leucine zipper proteins compete for the G-box-like element TGACGTGG. Plant Cell **4:** 1309–1319

Shi CL, Stenvik GE, Vie AK, Bones AM, Pautot V, Proveniers M, Aalen RB, Butenko MA (2011) *Arabidopsis* class I KNOTTED-like homeobox proteins act downstream in the IDA-HAE/HSL2 floral abscission signaling pathway. Plant Cell **23:** 2553–2567

Sieburth LE, Meyerowitz EM (1997) Molecular dissection of the *AGAMOUS* control region shows that *cis* elements for spatial regulation are located intragenically. Plant Cell **9:** 355–365

Smith HM, Campbell BC, Hake S (2004) Competence to respond to floral inductive signals requires the homeobox genes *PENNYWISE* and *POUND-FOOLISH*. Curr Biol **14:** 812–817

Smith HM, Hake S (2003) The interaction of two homeobox genes, *BREVIPEDICELLUS* and *PENNYWISE*, regulates internode patterning in the *Arabidopsis* inflorescence. Plant Cell **15:** 1717–1727

Smith HM, Ung N, Lal S, Courtier J (2011) Specification of reproductive meristems requires the combined function of SHOOT MERISTEMLESS and floral integrators FLOWERING LOCUS T and FD during Arabidopsis inflorescence development. J Exp Bot **62:** 583–593

Smyth DR, Bowman JL, Meyerowitz EM (1990) Early flower development in *Arabidopsis*. Plant Cell **2:** 755–767

Smyth GK (2005) Limma: linear models for microarray data. *In* RC Gentleman, VJ Carey, S Dudoit, R Irizarry, W Huber, eds, Bioinformatics and Computational Biology Solutions Using R and Bioconductor. Springer, New York, pp 397–420

Srikanth A, Schmid M (2011) Regulation of flowering time: all roads lead to Rome. Cell Mol Life Sci **68:** 2013–2037

Stief A, Altmann S, Hoffmann K, Pant BD, Scheible WR, Bäurle I (2014) *Arabidopsis* miR156 regulates tolerance to recurring environmental stress through SPL transcription factors. Plant Cell **26:** 1792–1807

Sun S, Yu JP, Chen F, Zhao TJ, Fang XH, Li YQ, Sui SF (2008) TINY, a dehydration-responsive element (DRE)-binding protein-like transcription factor connecting the DRE- and ethylene-responsive element-mediated signaling pathways in Arabidopsis. J Biol Chem **283:** 6261–6271

Teper-Bamnolker P, Samach A (2005) The flowering integrator FT regulates *SEPALLATA3* and *FRUITFULL* accumulation in *Arabidopsis* leaves. Plant Cell **17:** 2661–2675

Tian C, Zhang X, He J, Yu H, Wang Y, Shi B, Han Y, Wang G, Feng X, Zhang C, et al (2014) An organ boundary-enriched gene regulatory network uncovers regulatory hierarchies underlying axillary meristem initiation. Mol Syst Biol **10:** 755

Ung N, Lal S, Smith HMS (2011) The role of PENNYWISE and POUND-FOOLISH in the maintenance of the shoot apical meristem in Arabidopsis. Plant Physiol **156:** 605–614

Ung N, Smith HMS (2011) Regulation of shoot meristem integrity during Arabidopsis vegetative development. Plant Signal Behav **6:** 1250–1252

Wang JW (2014) Regulation of flowering time by the miR156-mediated age pathway. J Exp Bot **65:** 4723–4730

Wang JW, Czech B, Weigel D (2009) miR156-regulated SPL transcription factors define an endogenous flowering pathway in *Arabidopsis thaliana*. Cell **138:** 738–749

Wasternack C, Hause B (2013) Jasmonates: biosynthesis, perception, signal transduction and action in plant stress response, growth and development. An update to the 2007 review in Annals of Botany. Ann Bot (Lond) **111:** 1021–1058

Wasternack C, Kombrink E (2010) Jasmonates: structural requirements for lipid-derived signals active in plant stress responses and development. ACS Chem Biol **5:** 63–77

Wigge PA, Kim MC, Jaeger KE, Busch W, Schmid M, Lohmann JU, Weigel D (2005) Integration of spatial and temporal information during floral induction in Arabidopsis. Science **309:** 1056–1059

Wild M, Achard P (2013) The DELLA protein RGL3 positively contributes to jasmonate/ethylene defense responses. Plant Signal Behav **8:** e23891

Wild M, Davière JM, Cheminant S, Regnault T, Baumberger N, Heintz D, Baltz R, Genschik P, Achard P (2012) The *Arabidopsis* DELLA *RGA-LIKE3* is a direct target of MYC2 and modulates jasmonate signaling responses. Plant Cell **24:** 3307–3319

Wu G, Park MY, Conway SR, Wang JW, Weigel D, Poethig RS (2009) The sequential action of miR156 and miR172 regulates developmental timing in Arabidopsis. Cell **138:** 750–759

Wu G, Poethig RS (2006) Temporal regulation of shoot development in *Arabidopsis thaliana* by *miR156* and its target *SPL3*. Development **133:** 3539–3547

Xiang D, Venglat P, Tibiche C, Yang H, Risseeuw E, Cao Y, Babic V, Cloutier M, Keller W, Wang E, et al (2011) Genome-wide analysis reveals gene expression and metabolic network dynamics during embryo development in Arabidopsis. Plant Physiol **156:** 346–356

Xu M, Hu T, McKim SM, Murmu J, Haughn GW, Hepworth SR (2010) Arabidopsis BLADE-ON-PETIOLE1 and 2 promote floral meristem fate and determinacy in a previously undefined pathway targeting APETALA1 and AGAMOUS-LIKE24. Plant J **63:** 974–989

Yamaguchi A, Wu MF, Yang L, Wu G, Poethig RS, Wagner D (2009) The microRNA-regulated SBP-Box transcription factor SPL3 is a direct upstream activator of *LEAFY, FRUITFULL*, and *APETALA1*. Dev Cell **17:** 268–278

Yamaguchi S (2008) Gibberellin metabolism and its regulation. Annu Rev Plant Biol **59:** 225–251

Yang DL, Yao J, Mei CS, Tong XH, Zeng LJ, Li Q, Xiao LT, Sun TP, Li J, Deng XW, et al (2012) Plant hormone jasmonate prioritizes defense over growth by interfering with gibberellin signaling cascade. Proc Natl Acad Sci USA **109:** E1192–E1200

Yang L, Xu M, Koo Y, He J, Poethig RS (2013) Sugar promotes vegetative phase change in *Arabidopsis thaliana* by repressing the expression of *MIR156A* and *MIR156C*. eLife **2:** e00260

Yant L, Mathieu J, Dinh TT, Ott F, Lanz C, Wollmann H, Chen X, Schmid M (2010) Orchestration of the floral transition and floral development in *Arabidopsis* by the bifunctional transcription factor APETALA2. Plant Cell **22:** 2156–2170

Yu S, Cao L, Zhou CM, Zhang TQ, Lian H, Sun Y, Wu J, Huang J, Wang G, Wang JW (2013) Sugar is an endogenous cue for juvenile-to-adult phase transition in plants. eLife **2:** e00269

Yu S, Galvão VC, Zhang YC, Horrer D, Zhang TQ, Hao YH, Feng YQ, Wang S, Schmid M, Wang JW (2012) Gibberellin regulates the *Arabidopsis* floral transition through miR156-targeted SQUAMOSA promoter binding-like transcription factors. Plant Cell **24:** 3320–3332

Zhang Y, Turner JG (2008) Wound-induced endogenous jasmonates stunt plant growth by inhibiting mitosis. PLoS One **3:** e3699

Zhao M, Yang S, Chen CY, Li C, Shan W, Lu W, Cui Y, Liu X, Wu K (2015) Arabidopsis BREVIPEDICELLUS interacts with the SWI2/SNF2 chromatin remodeling ATPase BRAHMA to regulate *KNAT2* and *KNAT6* expression in control of inflorescence architecture. PLoS Genet **11:** e1005125

Zhu QH, Helliwell CA (2011) Regulation of flowering time and floral patterning by miR172. J Exp Bot **62:** 487–495